Gondwana Research 29 (2016) 83–104

Contents lists available at ScienceDirect

Gondwana Research

journal homepage: www.elsevier.com/locate/gr

GR Focus Review

The long-wavelength mantle structure and dynamics and implications for large-scale tectonics and volcanism in the Phanerozoic

Shijie Zhong [1], Xi Liu

Department of Physics, University of Colorado, Boulder, CO 80309, USA

ARTICLE INFO

Article history:
Received 21 March 2015
Received in revised form 17 July 2015
Accepted 26 July 2015
Available online 14 August 2015

Handling Editor: M. Santosh

Keywords:
Mantle seismic structure
Mantle dynamics
Supercontinent
Pangea
Large Igneous Provinces

ABSTRACT

The Earth's lower mantle structure, as revealed by seismic tomography studies, is best characterized by two large low seismic velocity provinces (i.e., LLSVP) beneath Africa and Pacific and their surrounding, circum-Pacific seismically fast anomalies. This mantle structure, sometimes called degree-2 structure, has been the most robust feature of all the seismic tomography models for the last 30 years. The dominantly degree-2 mantle structure explains the long-wavelength geoid anomalies including the geoid highs over Africa and Pacific. The LLSVPs are suggested to be the source regions for hotspot volcanism and large igneous province (LIP) events that are compositionally distinct from that for mid-ocean ridge basalts, thus holding the key to understanding mantle geochemistry. The degree-2 structure and LLSVPs have also been used as a reference frame to reconstruct paleogeography and true polar wander (TPW) history of the Earth for the Phanerozoic (i.e., for the last 500 Ma). This paper presents a comprehensive review of studies on the degree-2 mantle structure. While seismic tomography inversion and models are discussed, the main focus of the paper is on the dynamics of long-wavelength mantle convection, plate tectonics and large-scale volcanism. Important topics in the paper include: 1) the long-wavelength seismic structure for the present-day mantle, its possible relation to the long-wavelength geoid anomalies, volcanism and magmatism, and plate motion history, 2) the time evolution of the long-wavelength mantle structure in the Phanerozoic and its relations to Pangea assembly and breakup and history of volcanism/LIP events, and 3) the physics that controls the dynamics of long-wavelength mantle convection. The paper also provides a critical assessment on the validity of the hypothesis of spatially stationary Africa and Pacific LLSVPs since the early Paleozoic and its implications.

Contents

E-mail address: szhong@colorado.ed (S. Zhong).
[1] Tel.: +1 303 735 5095; fax: +1 303 492 7935.

http://dx.doi.org/10.1016/j.gr.2015.07.007
1342-937X/

1. Introduction

The first global seismic tomography model of the Earth's mantle was published about 30 years ago (Dziewonski, 1984; Woodhouse and Dziewonski, 1984) and it has profoundly shaped our understanding of the Earth's dynamics. The seismic model demonstrated that the Earth's lower mantle is characterized by two major seismically slow anomalies below Africa and Pacific that are surrounded by circum-Pacific seismically fast anomalies, i.e., a spherical harmonic degree-2 structure. This seismic imaging of the mantle has made it possible to integrate and understand a variety of observations including plate tectonics, long-wavelength gravity and topography anomalies, true polar wander, hotspot volcanism, and geochemical anomalies. It has also posed challenging questions to geodynamics regarding the origin and dynamics of such long-wavelength mantle structure. While the seismic structure represents a snapshot of the present-day Earth's mantle, recent studies have also started to explore time-evolution of mantle structure in Earth's geological history.

This paper presents a review of studies on long-wavelength mantle structure and its dynamics. This paper intends to address the following questions. What are the general characteristics of present-day's mantle structure as seen from seismic studies? What is the relationship between the long-wavelength, degree-2 mantle structure and hotspot volcanism and large igneous province events (LIP)? How is the long-wavelength mantle structure related to the positive gravity/geoid and residual topographic anomalies in the African and Pacific regions? What are the dynamic origins of and controls on the long-wavelength mantle structure? What are the possible scenarios of time evolution of mantle structure in the geological history? How can the time evolution of mantle structure be constructed and constrained? The paper is divided into three main sections. The first section is on the present-day mantle structure as seen in seismic tomography studies and its implications for other geophysical and geological observations and for geodynamics. The second section is on convection models of long-wavelength mantle structure. The third section discusses possible scenarios of time-evolution of long-wavelength mantle structure in recent geological history (i.e., since the early Paleozoic for the last 500 Million years) and its implications for the geological observations.

2. Long-wavelength Structure and Dynamics of the Present-day Earth's Mantle

2.1. Seismic observations of the long-wavelength mantle structure

Dziewonski (1984) and Woodhouse and Dziewonski (1984), published about 30 years ago, are the two seminal papers on the three-dimensional (3-D) structures of the Earth's mantle. In Dziewonski (1984), P-wave travel time residual data from the International Seismological Center (ISC) bulletins were used to construct a 3-D P-wave model for the lower mantle. In Woodhouse and Dziewonski (1984), surface wave seismograms from International Deployment of Accelerometers (IDA) and Global Digital Seismograph Network (GDSN) were used in waveform modeling to construct a 3-D S-wave model for the upper mantle. These models had relatively low resolution due to the limited data available at the time. The upper mantle S-wave model was represented by spherical harmonic functions up to degree and order 8 in the azimuthal directions (i.e., a resolution of ~5000 km) and by cubic polynomials in depth (i.e., a resolution of ~200 km) (Woodhouse and Dziewonski, 1984). The P-wave model for the lower mantle had up to degree and order 6 in spherical harmonics (i.e., a horizontal resolution of ~7000 km) and 4-th order Legendre functions in the radial direction (i.e., ~500 km resolution) (Dziewonski, 1984). Despite the coarse resolution, the upper mantle S-wave model showed clearly signatures of surface tectonic provinces: seismically fast anomalies in continental shields and slow anomalies beneath the mid-ocean ridges, which are consistent with early studies on regional scales (e.g., Brune and Dorman, 1963). Distinct features of the P-wave model for the lower mantle include the circum-Pacific fast speed anomalies from a depth of 1000 km to the core-mantle boundary (CMB), and slow speed anomalies below Africa and Pacific near the CMB (i.e., a spherical harmonic degree-2 structure) (Dziewonski, 1984). Although the upper mantle S-wave and lower mantle P-wave models employed entirely different techniques and data, the upper mantle and lower mantle structures showed some continuities from the upper to lower mantles (Woodhouse and Dziewonski, 1984).

Tanimoto (1990) constructed a 3-D global S-wave model for the whole mantle by using long-period body waves and surface waves, and the model was represented by 11 layers in the radial direction and spherical harmonics up to degree and order 6. The general characteristics of mantle structure in Tanimoto's model were consistent with those from Woodhouse and Dziewonski (1984) and Dziewonski (1984), for example, the association of mantle structure with surface tectonic settings. However, Tanimoto (1990) highlighted the predominance of the degree-2 structure throughout the mantle, although the power of seismic anomalies was relatively small in the mid-mantle, compared with that at shallow depths and near the CMB. The degree-2 lower mantle structure in the S-wave model in Tanimoto (1990) was similar to that revealed in the P-wave model in Dziewonski (1984). The degree-2 structure was also found to exist in the transition zone in a study of Earth's free oscillations and overtones (Masters et al., 1982). Remarkably, such a degree-2 mantle structure and its dominance in the mantle have been one of the most robust features in all the subsequent seismic tomography models that have employed larger datasets, higher resolutions and more advanced techniques (Su et al., 1994; Li and Romanowicz, 1996; Grand et al., 1997; Su and Dziewonski, 1997; van der Hilst et al., 1997; Ritsema et al., 1999; Masters et al., 2000; Grand, 2002; Montelli et al., 2004; Zhao, 2004; Panning and Romanowicz, 2006; Houser et al., 2008; Ritsema et al., 2011). This dominantly degree-2 mantle structure and its depth-dependent spectra are shown in Fig. 1a-c from a recent high-resolution S-wave model (Ritsema et al., 2011).

Although this paper focuses on the long-wavelength (e.g., degree-2) mantle structure, it is helpful to discuss briefly some general characteristics of the seismic models. More thorough reviews can be found in Thurber and Ritsema (2007), Romanowicz (2003) and Garnero (2000). Three different inversion approaches have been used, and they are to invert separately for P-wave and S-wave speed models (e.g., Dziewonski, 1984; Tanimoto, 1990) and jointly for S-wave, P-wave or bulk-sound speed models (e.g., Su and Dziewonski, 1997; Masters et al., 2000; Houser et al., 2008). These models have been parameterized using either mathematical basis functions (e.g., spherical harmonic functions or polynomials) (e.g., Dziewonski, 1984) or cells (e.g., Grand, 2002). The most recent high resolution S-wave model used spherical harmonics up to degree and order 40 (~1000 km horizontal resolution) (Ritsema et al., 2011) or cells with horizontal spacing of ~300 km (e.g., Grand, 2002; Houser et al., 2008), and had vertical resolution of ~150 km. Some recent P-wave models were parameterized in cells with horizontal spacing as small as ~100 km (Fukao and Obayashi, 2013).

The P-wave models, similar to Dziewonski et al. (1977), Dziewonski (1984), were constructed using the ISC and also hand-picked travel time data for direct arrivals, reflected phases and differential phases (e.g., P and PP). Due to the large number of data (e.g., ~10 million travel times in Fukao and Obayashi (2013)), the P-wave models tend to have high spatial resolution in well-sampled regions of the mantle, such as subduction zones, thus providing insights into associated physical processes such as subduction dynamics (e.g., Zhou, 1996; van der Hilst et al., 1997; Zhao, 2004). For example, some P-wave models suggest that subducted slabs might have stalled at least temporarily in the upper mantle or around ~1000 km depths (Fukao et al., 2001; Fukao and Obayashi, 2013), although some other slabs extend to the CMB (e.g., van der Hilst et al., 1997; Grand, 2002).

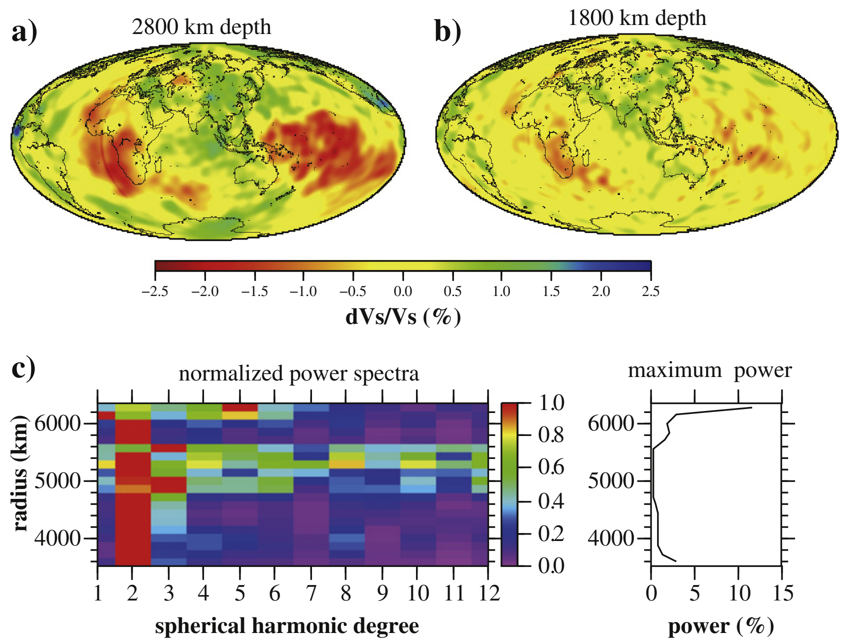

Fig. 1. Seismic structure at 2800 km (a) and 1800 km (b) depths and the normalized power spectra at different depths (c) from Ritsema et al. (2011). In Fig. 1c, the right panel shows the depth-dependence of maximum power that is used to normalize the power spectra for each depth. The major seismically slow anomalies beneath Africa and Pacific above the core-mantle boundary in Fig. 1a are often called the large low shear velocity provinces or LLSVPs. This figure shows clearly that the mantle structure is predominantly at degree-2.

The S-wave models often use long-period waveforms, in addition to travel times. The S-wave models have better resolution in oceanic upper mantle due to the sampling power of surface waves and in relatively hot or seismically slow regions of the mantle due to the high sensitivity of S-wave to temperature variations than the P-wave models (e.g., Romanowicz, 2003). For example, the S-wave models for the upper mantle clearly showed the thickening of oceanic lithosphere with distance from the mid-ocean ridges, thus helping illuminate dynamic processes affecting the evolution of oceanic lithosphere (e.g., Ritzwoller et al., 2004; Goes et al., 2013). The two major seismically slow anomalies in the bottom 100's of kilometers of the mantle beneath Africa and Pacific (i.e., now often called as the large low shear wave velocity provinces or LLSVP) (Fig. 1a), as the most important part of the degree-2 structure, are best seen in the S-wave models (e.g., Tanimoto, 1990; Su et al., 1994), although they were first reported in the P-wave model (Dziewonski, 1984). It should be pointed out that although different S-wave models show similar morphology for the LLSVPs, the detail may still differ significantly (e.g., Masters et al., 2000; Becker and Boschi, 2002; Panning and Romanowicz, 2006; Houser et al., 2008; Ritsema et al., 1999, 2011). The S-wave and bulk sound speed models from joint inversions will be discussed in a later section on possible large-scale chemical heterogeneities in the lower mantle.

2.2. Long-wavelength mantle structure, geoid anomalies, and the style of mantle convection

The 3-D seismic models have not only applications in seismology (e.g., more accurately locating earthquakes and predicting seismic wave propagation) but also implications for geodynamics. Generally speaking, mantle materials of the same composition with a slower seismic speed would have a higher temperature and a smaller density. Therefore, 3-D seismic structures of the mantle are expected to have implications for buoyancy and temperature fields in the mantle, hence the flow in the mantle and the gravity anomalies and volcanism at the Earth's surface. The 3-D seismic models also have implications for compositional structure of the mantle and the style of mantle convection (i.e., the whole mantle versus layered mantle convection).

There had been two competing models of the mantle as the global seismic models were being constructed in 1980's: the whole mantle convection and layered mantle convection (Fig. 2a-b) (e.g., Davies, 1984). The layered mantle convection model was mainly based on geochemical evidence such as isotopic difference between oceanic island basalts (OIB) and mid-ocean ridge basalts (MORB) (e.g., Hofmann, 1997), and the model stated that mantle convection would happen separately in the upper and lower mantles with insignificant mass exchange between them (Fig. 2b). In the whole mantle convection model, on the other hand, the upper and lower mantles form a single convective system with no significant barrier to flow in between (Fig. 2a). Seismic tomography models constructed in 1980's and the early 1990's provided strong support for the whole mantle convection (e.g., Davies and Richards, 1992). It was recognized that the circum-Pacific seismically fast anomalies in the lower mantle were closely associated with the past subduction zones (Dziewonski, 1984; Tanimoto, 1990; Su et al., 1994). High-resolution seismic models showed that subducted slabs extend to the lower mantle (e.g., van der Hilst et al., 1991; Grand, 1994; Grand et al., 1997), although as pointed out earlier, some recent studies suggested a rather complicated dynamics as the slabs descend to the CMB (Fukao and Obayashi, 2013). More discussions on this classic debate of the whole mantle convection versus layered mantle convection can be found in Davies (1999).

The early studies on 3-D global seismic models made attempts to explain the Earth's long-wavelength gravity/geoid anomalies (Dziewonski et al., 1977; Masters et al., 1982; Dziewonski, 1984). The geoid anomalies (i.e., the non-hydrostatic components of the gravitational potential anomalies) are predominated by their long-wavelength components with the degree-2 geoid that accounts for >50% of the total geoid power (Fig. 3a) (e.g., Lerch et al., 1983). The degree-2 geoid anomalies consist of equatorial positive geoid anomalies (i.e., degree $l = 2$ and order $m = 0$) and the two broad positive geoid anomalies over the Pacific and Africa (i.e., $l = 2$ and $m = 2$). The positive geoid anomalies correlate well with the two seismically slow anomalies beneath the Pacific and Africa in the lower mantle (i.e., LLSVPs) (Fig. 1)

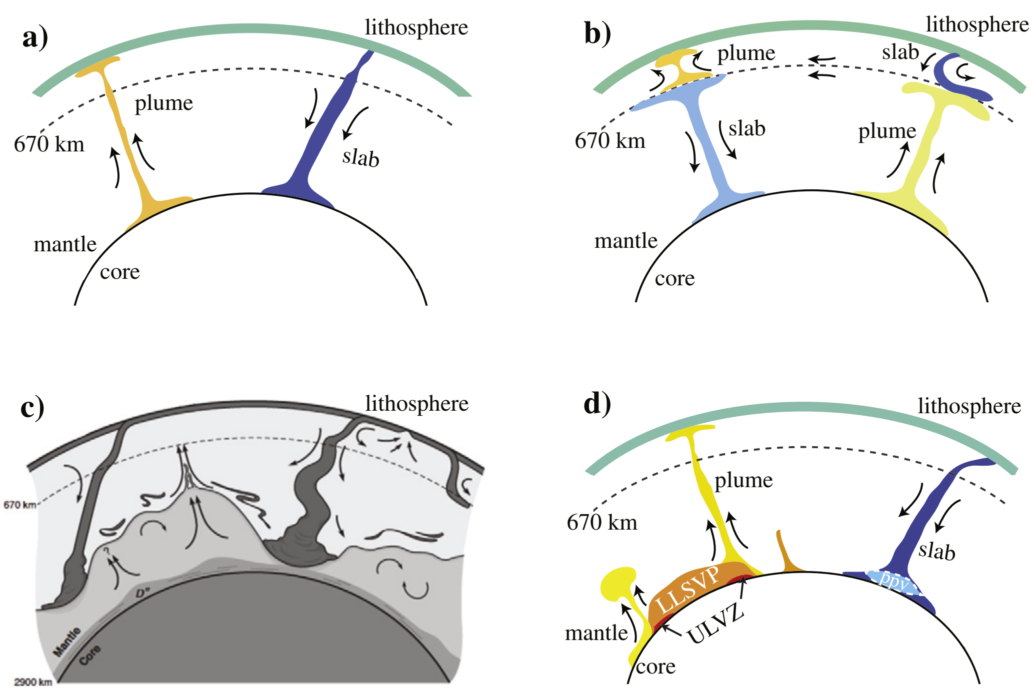

Fig. 2. Schematic diagrams showing different styles of mantle convection: an isochemical, whole mantle convection (a), a layered mantle convection with 670 km as the compositional boundary (b), a layered mantle convection by Kellogg et al. (1999) with an highly undulated compositional boundary at ~1700 km depth (c), and a mantle convection model with thermochemical piles (i.e., the LLSVPs), ULVZs, and pPv (d). Fig. 2c is taken from (Kellogg et al. 1999).

(e.g., Dziewonski, 1984; Tanimoto, 1990; Su et al., 1994; Ritsema et al., 2011). Hager et al. (1985) showed that the long-wavelength geoid anomalies could be explained in a whole mantle convection model with buoyancy force derived from the global seismic model (Dziewonski, 1984). In deriving buoyancy from seismic anomalies, a simple scaling relation is often assumed for a mantle with the same composition (i.e., the whole mantle convection), for example for S-wave model Vs, $\delta\rho/\rho = c\delta Vs/Vs$, where ρ is the density, and c is a conversion factor (Karato, 1993). In determining the geoid anomalies, such mantle flow models considered dynamic compensation effects of the mantle buoyancy at the surface and CMB, i.e., dynamic topography (Ricard et al., 1984; Richards and Hager, 1984). Since the dynamic compensation depends on mantle viscosity structure, the geoid anomalies have been used to constrain the lower mantle to be about two orders of magnitude more viscous than the upper mantle (e.g., Hager and Richards, 1989; Ricard et al., 1993). Besides explaining the long wavelength geoid, the dynamic models also predicted ~1 km dynamic topography highs in the central Pacific and Africa above the two LLSVPs, which is consistent with the inferred residual topography highs in these regions (e.g., Davies and Pribac, 1993; Nyblade and Robinson, 1994; Lithgow-Bertelloni and Silver, 1998). The success of the dynamic geoid models provided further support for the whole mantle convection (Hager and Richards, 1989).

2.3. LLSVPs as large-scale chemical heterogeneities and the style of mantle convection

By the mid-1990's, with the clear association of seismically imaged fast speed anomalies in the lower mantle with subduction zones at the surface and the success of the dynamic flow models for the geoid, the whole mantle convection at least on the large scale had become widely accepted in geodynamics (e.g., Davies and Richards, 1992). However, it remained unclear how the whole mantle convection could be reconciled with some of the geochemical observations. For example, the isotopic difference between OIB and MORB may require different, isolated source regions or reservoirs in the mantle, and the reservoir for OIB may represent enriched and possibly primitive mantle (e.g., Hofmann, 1997). The concentration of ^{40}Ar in the Earth's atmosphere may imply that only some fraction of the mantle has been processed or molten by the tectonic and volcanic processes (e.g., Allegre et al., 1983, 1996). The whole mantle convection, if operating for the entire history of the Earth, would have homogenized and processed the whole mantle, thus making it difficult to account for the geochemical observations (van Keken and Ballentine, 1999).

Kellogg et al. (1999) proposed a new layered-mantle model attempting to reconcile the seismic and geochemical observations (Fig. 2c). The model was partly motivated by the apparent disappearance or weakening of fast P-wave anomalies (i.e., subducted slab signals) at a depth of ~1700 km (Karason and van der Hilst, 1999). Although the bottom layer (i.e., for the more primitive and less processed mantle) in Kellogg et al.'s model had a smaller volume than that in the conventional layered mantle model, it might still be sufficient to explain the geochemical observations in mass balance calculations. In this model, the intrinsic density increase across the compositional boundary was relatively small such that the boundary would have 100's km topography (Fig. 2c), making it difficult to be detected seismically (Kellogg et al., 1999). Although seismic studies searching for such a layered mantle structure did not produce any confirmation (e.g., Castle and van der Hilst, 2003), Kellogg et al.'s model inspired new lines of thinking for the structure and dynamics of the mantle.

In the late 1990's and early 2000's, a number of seismic studies indicated that the LLSVPs in the bottom 400 km of the lower mantle might be compositionally distinct from the rest of the mantle (e.g., Masters et al., 2000; Wen et al., 2001). The joint inversion studies for P-, S- and bulk sound speeds showed that S-wave and bulk sound speed anomalies were anti-correlated in the African and Pacific LLSVPs (Su and Dziewonski, 1997; Kennett et al., 1998; Masters et al., 2000). This anti-correlation was suggested to result from compositional difference between the LLSVPs and the ambient mantle (Masters et al., 2000). A normal mode study suggested that the density in the LLSVPs might be higher than the ambient mantle (Ishii and Tromp, 1999), although the

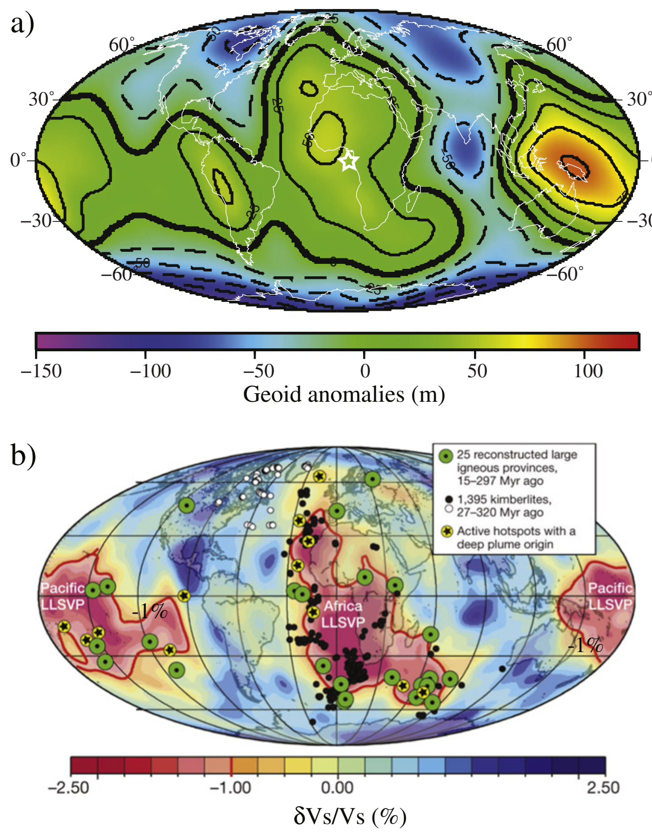

Fig. 3. A map of earth's non-hydrostatic geoid anomalies from degrees 2 to 12 (a), and spatial distribution of hotspot volcanism with deep mantle plumes and restored LIP eruption sites plotted on a map of seismic anomalies at 2800 km depth from Smean model (Becker and Boschi, 2002) (b). In Fig. 3a, the star at (0°N, 11°E) marks the axis going through the centers of the positive degree-2 geoid anomalies associated with the African and Pacific LLSVPs. This axis defines the great circle path along which the Earth's spin axis migrates for TPW events inferred in Torsvik et al. (2010, 2014). Fig. 3b is taken from Torsvik et al. (2010). In addition to hotspot volcanism and LIPs, Fig. 3b also shows the distribution of kimberlites (black and white dots) and -1% contours of S-wave velocity anomalies (red contours) that were often used to define the LLSVPs.

uniqueness of this result was challenged (Resovsky and Ritzwoller, 1999). Waveform studies for seismic waves grazing along the edges of the African LLSVP found that the seismic wave speeds might vary too rapidly (e.g., ~3% over 50 km distance) there to be explained by thermal anomalies alone, suggesting a compositional difference between the LLSVP and the ambient mantle (Wen et al., 2001; Ni et al., 2002; Wang and Wen, 2004). Similar inferences were made for the Pacific LLSVP, although the Pacific LLSVP may be more heterogeneous than the African LLSVP (He and Wen, 2009, 2012).

It is important to point out that the CMB region (i.e., the D" region) is rather complicated based on seismic and mineral physics studies (see Garnero and McNamara (2008) for a review). It has been proposed that in addition to the possibly chemically distinct African and Pacific LLSVPs, there are two other seismically distinct features. First, an endothermic phase change of perovskite to post-perovskite exists ~300 km above the CMB in mostly seismically fast regions (i.e., underneath the circum-Pacific subduction) (Sidorin et al., 1999; Murakami et al., 2004; Lay and Garnero, 2007) and causes a sharp seismic discontinuity (Lay and Helmberger, 1983). Second, ultra-low velocity zones (ULVZ) with a thickness of tens of kilometers exist as isolated patches immediately above the core and mostly below the LLSVPs (Lay et al., 1998; Garnero, 2000; Garnero and McNamara, 2008). The ULVZ must be chemically distinct and may be associated with partial melting or enriched in Fe (Garnero and McNamara, 2008). However, this paper's emphasis is on the large-scale feature of the LLSVPs, and the detail discussions on the ULVZ and perovskite to post-perovskite phase change can be found in Garnero and McNamara (2008).

Therefore, a new thermochemical mantle model as a revision from Kellogg et al. (1999) would have the Pacific and African LLSVPs as chemically distinct, heavy reservoirs or thermochemical piles (Fig. 2d) (e.g., Boyet and Carlson, 2005; McNamara and Zhong, 2005a; Garnero and McNamara, 2008). The volume of the LLSVPs was estimated to be ~2% of the mantle (Hernlund and Houser, 2008; He and Wen, 2009). Many questions remain unanswered about this model, including the origin of the chemical heterogeneities (i.e., the LLSVPs) and how the model accounts for geochemical observations. For example, are the LLPSVs the residue of early Earth differentiation processes (e.g., a basal magma ocean (Labrosse et al., 2007) or overturn of cumulates following solidification of shallow magma ocean cumulates (Boyet and Carlson, 2005) or the recycled oceanic crust (Christensen and Hofmann, 1994; Li et al., 2014; Nakagawa and Tackley, 2014)? With the small volume and mass for the LLSVPs, would this model adequately account for the geochemical observations of the difference between OIB and MORB and other noble gases (Hofmann, 1997; Gonnermann and Mukhopadhyay, 2009; Tucker et al., 2012)?

Finally, it should be pointed out that some studies have indicated that the classic, isochemical whole-mantle convection model, if considering the perovskite to post-perovskite phase change and mantle subadiabaticity, may account for all the seismic observations including the anti-correlation between the shear wave and bulk sound speed anomalies with no need for large-scale chemical heterogeneities (e.g., Bunge et al., 2001; Bunge, 2005; Schuberth et al., 2009; Davies et al., 2012; Schuberth et al., 2012). For example, Schuberth et al. (2009) suggested that isochemical whole-mantle convection models could produce large horizontal gradient in shear wave speeds immediately above the CMB at 2800 km depth that might explain the seismic observations of the African LLSVP (Wen et al., 2001; Ni et al., 2002). However, it should be pointed that the large horizontal gradient associated with the African seismic anomalies occurs at much shallower depths (~2000-2400 km) (Wen et al., 2001; Ni et al., 2002) where isochemical whole-mantle convection models seem to produce much smaller horizontal variations (Schuberth et al., 2009). Nevertheless, it remains an important subject of studies to determine to what extent the LLSVPs are chemically heterogeneous.

2.4. Hotspot volcanism, mantle plumes and the LLSVPs

Hotspot volcanism has had a unique global significance in geodynamics (e.g., Davies, 1999). Hotspot tracks and volcanism ages have helped constrain global plate motion and provide a reference frame for plate motions (e.g., Gordon and Jurdy, 1986). The sources for hotspot volcanism appear relatively stationary with respect to each other and are often thought to be mantle plumes that ascend from the deep mantle and possibly the CMB region (Morgan, 1971). The plume model helps explain the formation of not only hotspot volcanism but also large igneous provinces (LIP) (e.g., Campbell and Griffiths, 1990; Richards et al., 1991; Hill et al., 1992). Topographic swells associated with hotspots have also been used to constrain buoyancy flux and heat flux of mantle plumes that are interpreted as a measure of heat flux out of the core (Davies, 1988a; Sleep, 1990).

Chase (1979) noticed that the hotspots were preferentially located in regions with long-wavelength positive geoid (e.g., the central Pacific and African regions) (Fig. 3a and b). Anderson (1982) proposed that the upper mantle in the central Pacific and Africa might be relatively hot due to supercontinent Pangea's insulation effect, and the hot mantle would produce the positive geoid anomalies and hotspot volcanism at the surface. The global seismic models (e.g., Dziewonski, 1984; Ritsema et al., 2011) showed that the mantle beneath Africa and Pacific is indeed seismically slow and likely hot, but mainly at large depths in the lower mantle (i.e., the LLSVPs), not as much in the upper mantle as proposed by Anderson (1982). In their dynamic geoid models, Hager et al. (1985) demonstrated that such lower mantle buoyancy structures were critical to produce the positive dynamic topography and geoid at the surface and broad mantle upwellings in the central Pacific and Africa. Therefore, Hager et al. (1985) suggested that the hotspot volcanism might be related to the African and Pacific LLSVPs (Fig. 3b). It should also be noted that Anderson (1982) proposed that the true polar wander (TPW), by aligning the maximum moment of inertia axis with the spin axis, would play a role in causing the geoid highs and hotspots near the equator.

However, due to the small radius and transient dynamics of mantle plumes (e.g., Campbell and Griffiths, 1990; Zhong et al., 2000a; Lithgow-Bertelloni et al., 2001), it is challenging to image the plumes in seismic studies (e.g., Montelli et al., 2004; Wolfe et al., 2009). This makes it difficult to examine any possible relation between hotspot volcanism and deep mantle processes and structures including the LLSVPs (Courtillot et al., 2003). However, some interesting spatial correlations between hotspots/LIPs and the LLSVPs have been noticed (Davaille, 1999; Jellinek and Manga, 2004). Thorne et al. (2004) suggested that hotspots, if projected vertically down into the D" regions, tended to occur in regions where seismic speeds vary more rapidly in the LLSVPs. Torsvik et al. (2006, 2010) proposed that after being restored to their original eruption sites using plate motion history models, the LIPs of the last ~300 Myrs would appear to occur mostly along the edges of the LLSVPs as defined by -1% contour level in an averaged S-wave model, Smean (Becker and Boschi, 2002) (Fig. 3b). However, the statistical significance of the correlation of LIPs with the edges of the LLSVPs has been questioned (Davies et al., 2015; Austermann et al., 2015).

Although the spatial correlation of hotspot volcanism and the LLSVPs was recognized in 1980's (e.g., Anderson, 1982; Hager et al., 1985), its significance had not been fully explored in geodynamics possibly for two reasons. First, the disparity of length scales between the LLSVPs (i.e., ~10,000 km) and plumes (i.e., ~100's km) makes it difficult to model their dynamic interaction (e.g., Zhong et al., 2000a). Second, it was suggested that mantle plumes might only transfer a small fraction (~10%) of convective heat flux out of the Earth's mantle, hence not as important from the global energetics point of view (e.g., Davies, 1999). Plume heat flux inferred from swell topography at hotspots was ~3.5 TW or ~10% of the Earth's total convective heat flux (Davies, 1988a; Sleep, 1990; Hill et al., 1992). The plume heat flux was considered to represent the heat flux out of the core (i.e., the cooling of the core). This suggests that mantle convection would be mainly driven by the internal heating (i.e., radiogenic heating and secular cooling of the mantle) with an internal heating ratio at ~90% (Davies, 1988a; Sleep, 1990) and that the cold downwellings should be the primary heat transfer agent and structure in the mantle (e.g., Davies, 1999). Indeed, mantle buoyancy models were constructed by including subducted slabs over the last 120 Myr and ignoring any active mantle upwellings such as the LLSVPs, and such buoyancy models were used to successfully model the geoid and mantle flow (Ricard et al., 1993; Lithgow-Bertelloni and Richards, 1998).

However, our understanding of plume dynamics and the core heat flux has evolved significantly in the last ten years. Recent studies suggest that the core heat flux should be significantly larger than previously estimated and that the mantle upwelling structures including the LLSVPs play an important role in the dynamics of the lower mantle. Recent mineral physics studies indicate that the thermal conductivity of the core materials is probably three times larger than previously estimated, and that the core heat flux is ~15 TW (de Koker et al., 2012; Pozzo et al., 2012; Gomi et al., 2013), although smaller thermal conductivity is also suggested (Zhang et al., 2015). Seismic observations of the post-perovskite phase change, together with mineral physics studies on its Clapeyron slope, constrain the CMB heat flux at 10-16 TW (Hernlund et al., 2005; Lay et al., 2006; van der Hilst et al., 2007; Lay et al., 2008; Hernlund, 2010). For a review on the core heat flux, see Hernlund and McNamara (2015).

Can the large core heat flux be made compatible with the much smaller plume heat flux inferred from observations and its implied dynamic state of the D" regions (e.g., Davies, 1999)? It has been suggested that the plume heat flux does not represent the core heat flux based on simplified convection models (in either Cartesian, cylindrical geometry or 2-D) (Labrosse, 2002; Yoshida and Ogawa, 2005; Mittelstaedt and Tackley, 2006). However, 3-D spherical models of mantle convection with realistic mantle rheology showed that the plume heat flux immediately above the CMB represented 80-90% of the core heat flux using (Zhong, 2006; Leng and Zhong, 2008), thus confirming the proposal by Davies (1988a) and Sleep (1990). These model calculations also demonstrated that due to excessive adiabatic cooling for hot plumes, the plume heat flux would decrease by about three times as plumes ascend from the D" to the upper mantle. Taking the plume heat flux in the upper mantle to be 3.5 TW as constrained by swell topography, these studies suggest that the CMB heat flux would be ~12 TW or ~35% of the total convective heat flux at the Earth's surface (Zhong, 2006; Leng and Zhong, 2008), consistent with the other estimates discussed earlier. Bunge (2005) reported that plume excess temperature near the CMB region is significantly larger than that in the upper mantle in 3-D spherical models of mantle convection due to mantle sub-adiabaticity (Bunge et al., 2001), and suggested that CMB heat flux could be significantly larger than that inferred from swell topography. By quantifying plume heat flux, Leng and Zhong (2008) found that mantle sub-adiabaticity may indeed account for ~25% of plume heat flux reduction from the CMB to the upper mantle, but excessive adiabatic cooling of hot plumes is the most important for the plume heat flux reduction. Importantly, the large CMB heat flux suggests that the large-scale seismically slow anomalies in the lower mantle including the LLSVPs are significant for the dynamics of mantle plumes and heat transfer, and that the LLSVPs may contain significant thermal component.

3. Dynamic Models for Long-wavelength Mantle Structure

The long-wavelength (i.e., predominantly degree-2) mantle structure revealed in seismic tomography and its spatial correlation with the geoid, topography, and hotspot volcanism suggest the importance of long-wavelength mantle dynamic processes. An important goal in geodynamics has been to understand the origin of the long-wavelength mantle structure and its relation to surface observables. However, the dynamics of the mantle is very complicated with temperature- and pressure-dependent thermodynamic parameters and non-linear viscosity. The Rayleigh number for the mantle that measures convective vigor is supercritical by possibly 4 orders of magnitude, leading to thin top and bottom thermal boundary layers and narrow upwellings and downwellings. To deal with these challenges, geodynamic models are often formulated with assumptions and simplifications with a goal to understand the key dynamic process. For understanding the long-wavelength mantle structure, two classes of mantle convection models have been formulated: semi-dynamic and fully dynamic models. The semi-dynamic models use prescribed plate motions as surface boundary conditions, while the fully dynamic models employ free-slip or free-stress boundary conditions without imposing any kinematic constraints. In this section, we will first review semi-dynamic and full dynamic models that have been built for understanding the long-wavelength mantle structure for the present-day Earth's mantle. We will also discuss dynamic models for time-evolution of mantle structure in the Phanerozoic.

3.1. Semi-dynamic models for seismic structures of the mantle

It was recognized in one of the first global mantle flow models that plate motions as imposed surface boundary conditions have important controls on mantle flow patterns (e.g., Hager and O'Connell, 1979). Beneath surface plate convergence (divergence) is mantle downwelling (upwelling) flow. Although these early models did not solve for time-dependent mantle structures, subsequent time-dependent 2-D convection models using velocity boundary conditions (i.e., semi-dynamic models) showed similar effects of plate motions on mantle flow and temperature structures (e.g., Davies, 1988b). Semi-dynamic models have a number of advantages, mostly in linking surface observations with mantle dynamics. For example, semi-dynamic models with imposed plate motions help understand the dynamics of lithospheric instability and its effects on the ocean-depth and age relationship (e.g., Huang and Zhong, 2005). Semi-dynamic models of mantle convection with plate motion history may help understand the origin of seismic mantle structure, as done on a global scale (e.g., Bunge et al., 1998) and also on regional scales for the western US (e.g., Liu et al., 2008; Liu and Stegman, 2012) and Alaska subduction zone (e.g., Jadamec and Billen, 2010).

Semi-dynamic models of uniform composition (i.e., isochemical or purely thermal models of mantle convection) using plate motion history for the last 120 Myrs (Lithgow-Bertelloni and Richards, 1998) as surface boundary conditions (Fig. 4a-b) reproduced well the circum-Pacific seismically fast structure (i.e., subducted slabs), although they had only some limited success in explaining the large-scale seismically slow structures (i.e., LLSVPs) (Bunge et al., 1998, 2002). Recently, similar isochemical, semi-dynamic models showed improved fit to the LLSVP structures and were used to explain the LLSVPs as purely thermal origins without revoking chemical heterogeneities (Schuberth et al., 2009; Davies et al., 2012). The lower mantle viscosity in these models is about 10^{23} Pas, and this probably represents the upper bound of the lower mantle viscosity inferred from post-glacial rebound studies (Simons and Hager, 1997; Mitrovica and Forte, 2004) that may still have rather limited constraining power on mantle viscosity profiles (e.g., Paulson et al., 2007).

Including chemically dense materials with a volume similar to that inferred seismically for the LLSVPs (i.e., ~2% of the total mantle volume) (Hernlund and Houser, 2008; He and Wen, 2012), the semi-dynamic models reproduced both the African and Pacific LLSVPs and the circum-Pacific downwelling structures (Fig. 5) (McNamara and Zhong, 2005a; Bull et al., 2009; Bower et al., 2013) with a wide range of lower mantle viscosity (Zhang et al., 2010), consistent with the seismic studies that suggest for a chemical origin of the LLSVPs (e.g., Masters et al., 2000; He and Wen, 2012). These thermochemical semi-dynamic models showed that the volume and intrinsic density of the chemically distinct materials above the CMB played an important role in forming the LLSVPs (e.g., Zhang et al., 2010). Generally speaking, the larger the density difference between the chemically distinct materials and the normal mantle is, the less undulating the compositional interface is. When either the density difference or the volume of the dense material is too large, the CMB would not be exposed to cold downgoing slabs (McNamara and Zhong, 2005a; Zhang et al., 2010), making it difficult to explain the presence of the post-perovskite phase changes (e.g., Hernlund et al., 2005) and the LLSVPs. However, the density difference cannot be too small either, in order to keep the LLSVPs stable in the deep mantle against gravitational overturn. Another factor affecting the thermochemical structure is convective vigor or Rayleigh number (e.g., Tackley, 1998; McNamara and Zhong, 2004).

The semi-dynamic models utilize the observed plate motions to make model predictions that could be tested against observations of seismic structure (e.g., Bunge et al., 1998; McNamara and Zhong, 2005a,b; Bull et al., 2009; Schuberth et al., 2009), dynamic topography, and heat flux (e.g., Zhang and Zhong, 2011; Zhang et al., 2012; Flament et al., 2013), and they have been a powerful tool in geodynamic studies. However, these models have a number of disadvantages. First, they do not really provide any mechanistic explanation on the formation of the long-wavelength plate motions, although the models predict the long-wavelength mantle structure using the imposed plate motions. This topic will be discussed in the next sub-section. Second, caution must be exercised to avoid introducing excessive kinematic energy and dissipation from the imposed plate motions to the convective system (e.g., Davies, 1989; King et al., 1992; Han and Gurnis, 1996). One possible practice is to choose Rayleigh number such that the magnitudes of flow velocity and heat flux from convection models with free-slip boundary conditions approximately match that from the semi-dynamic models at the same Ra (McNamara and Zhong, 2005a; Zhang et al., 2010).

While the preceding two issues were discussed previously in literature, the third difficulty with the semi-dynamic models was only recently recognized and is related to the dynamic consistency of plate motion reference frames (i.e., net rotation of lithosphere) with model viscosity structure (Rudolph and Zhong, 2014). Plate motion models are often given in a hotspot reference frame and they often have significant net rotation of lithosphere relative (e.g., Gordon and Jurdy, 1986). When they are used as surface boundary conditions in semi-dynamic models, depending on mantle viscosity structure (i.e., the lateral variations in viscosity), modeled differential rotation between lithosphere and the mantle may not be sufficient to match with what is implied in the plate motion models, as known in dynamic models for the present-day plate motions (e.g., Ricard et al., 1991; Zhong, 2001; Becker, 2006, 2008; Conrad and Behn, 2010; Gerault et al., 2012). Rudolph and Zhong (2014) found that with thick continental keels, the modeled differential rotation of lithosphere would match that in plate motion model of Seton et al. (2012) for the last 25 Myrs, but not for early time periods especially when the net rotation is larger than 0.5°/Myr. Such a deficiency may not affect previous results on the long-wavelength (e.g., degrees 1 and 2) mantle structures, but its effects on mantle plume trajectories and such defined plate motions (e.g., Steinberger and O'Connell, 2000; O'Neill et al., 2005) remain unclear (Rudolph and Zhong, 2014). The effects of plate motion reference frames on mantle structure have been explored in Shephard et al. (2012).

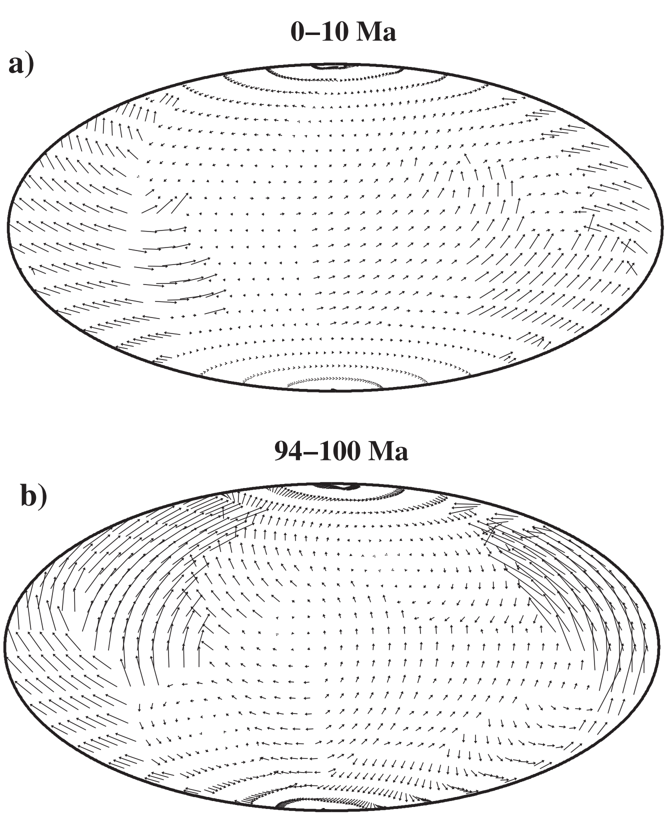

Fig. 4. Plate motion at the present-day (a) and ~100 Ma (b) from Lithgow-Bertelloni and Richards (1998).

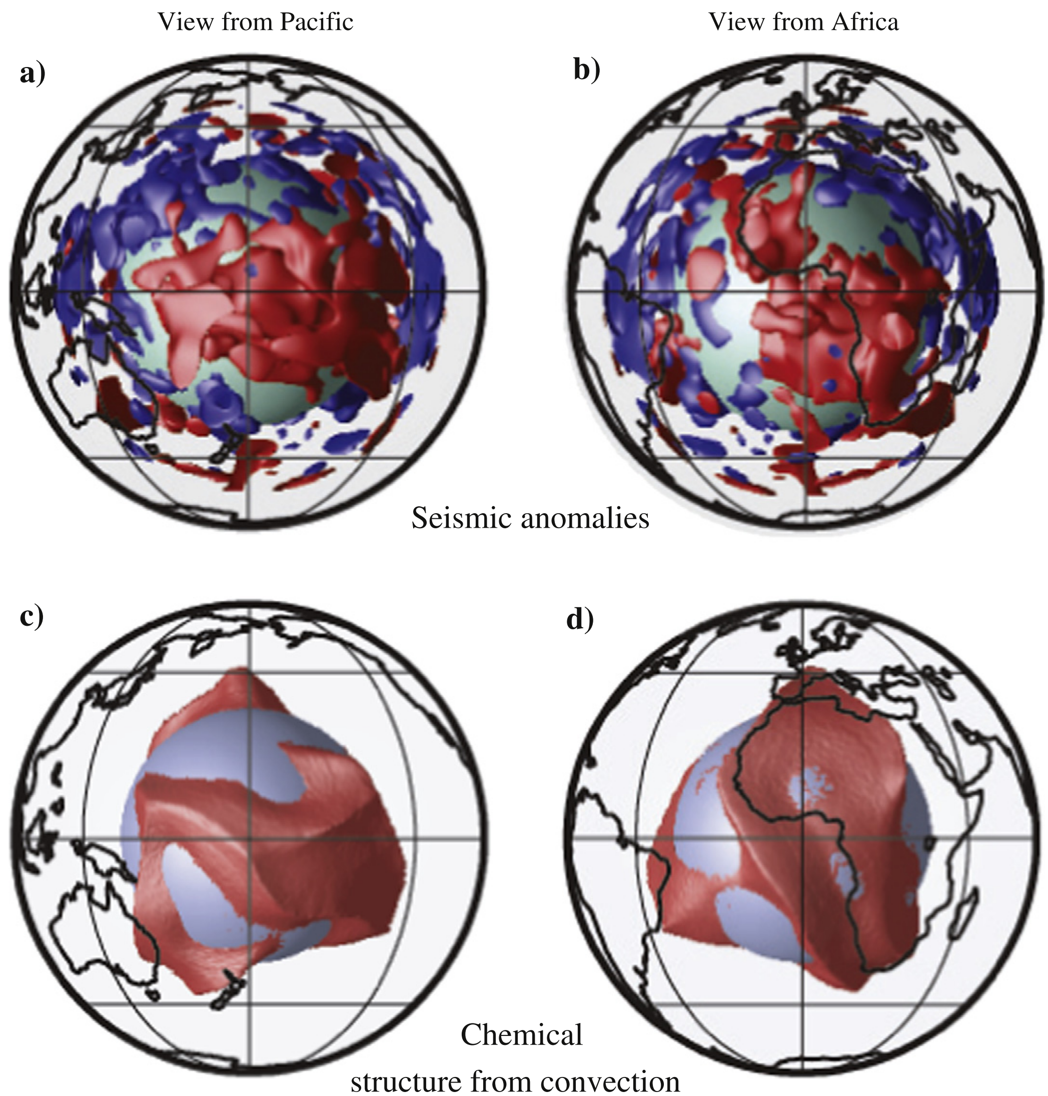

Fig. 5. Seismic model of Ritsema et al. (2004) viewed from above the Pacific (a) and Africa (b), and the chemical structure from 3-D semi-dynamic models of thermochemical convection by McNamara and Zhong (2005a) viewed from above the Pacific (c) and Africa (d). In Fig. 5a-b, only the seismic models below 1100 km depth are shown, and the red and blue iso-surfaces represent seismically slow and fast anomalies. Fig. 5c-d show iso-surfaces for compositional field that represent the chemically distinct and dense mantle or LLSVPs. The figure was modified from McNamara and Zhong (2005a).

3.2. Fully dynamic models – numerical modeling results

If one postulates that plate tectonics emerges from mantle convection with surface plates as the cold and stiff convective boundary layer at the surface, then an ultimate answer to the long-wavelength mantle structure must reside in the dynamics of mantle convection without imposed surface plate motions (e.g., Bercovici, 2003). Indeed, convective wavelength and structure has been extensively studied in dynamically self-consistent mantle convection models in the last 30 years. These studies (Jaupart and Parsons, 1985; Bercovici et al., 1989a,b; Tackley, 1993; Tackley et al., 1993; Zhong and Gurnis, 1993; Zhang and Yuen, 1995; Bunge et al., 1996; Tackley, 1996a; McNamara and Zhong, 2005b; Yoshida and Kageyama, 2006; Zhong et al., 2007) have revealed that the most important controlling parameter on convective wavelength is the mantle viscosity structure, while other relevant parameters include Rayleigh number (Ra), endothermic phase change, and mantle compressibility.

Early 3-D global dynamic convection models using a spectral method were computed for constant viscosity at a relatively small Ra due to computational limitations (note that thin thermal boundary layers for large Ra convection would require high numerical resolution and more computational resources) (e.g., Bercovici et al., 1989a,b). These studies showed that at Ra less than ten times of the critical Ra, convection would form stable either cubic or tetrahedral pattern (i.e., degrees 3 or 4) (Fig. 6a). Convection at a larger Rayleigh number and/or with internal heating would have time-dependent convective structures of shorter wavelengths with sheet-like downwelling and cylindrical upwelling structures (e.g., Bercovici et al., 1989b) (Fig. 6b). While the downwelling and upwelling structures resemble subducted slabs and mantle plumes, convective structure from the constant viscosity convection models has much shorter wavelengths than the degree-2 for the Earth's mantle (Tackley et al., 1993; Bunge et al., 1996; Zhong et al., 2000a, 2008).

Introducing depth-dependent thermal conductivity and coefficient of thermal expansion, and mantle compressibility would help increase convective wavelengths (e.g., Hansen et al., 1993; Zhang and Yuen, 1995; Yoshida and Santosh, 2011). An endothermic phase change from spinel to post-spinel that corresponds to the 670-km seismic discontinuity was found to increase convective wavelengths in global compressible mantle convection models with constant viscosity at modest Rayleigh number (Tackley et al., 1993). However, this effect is only significant for relatively large Clapeyron slope of the phase change

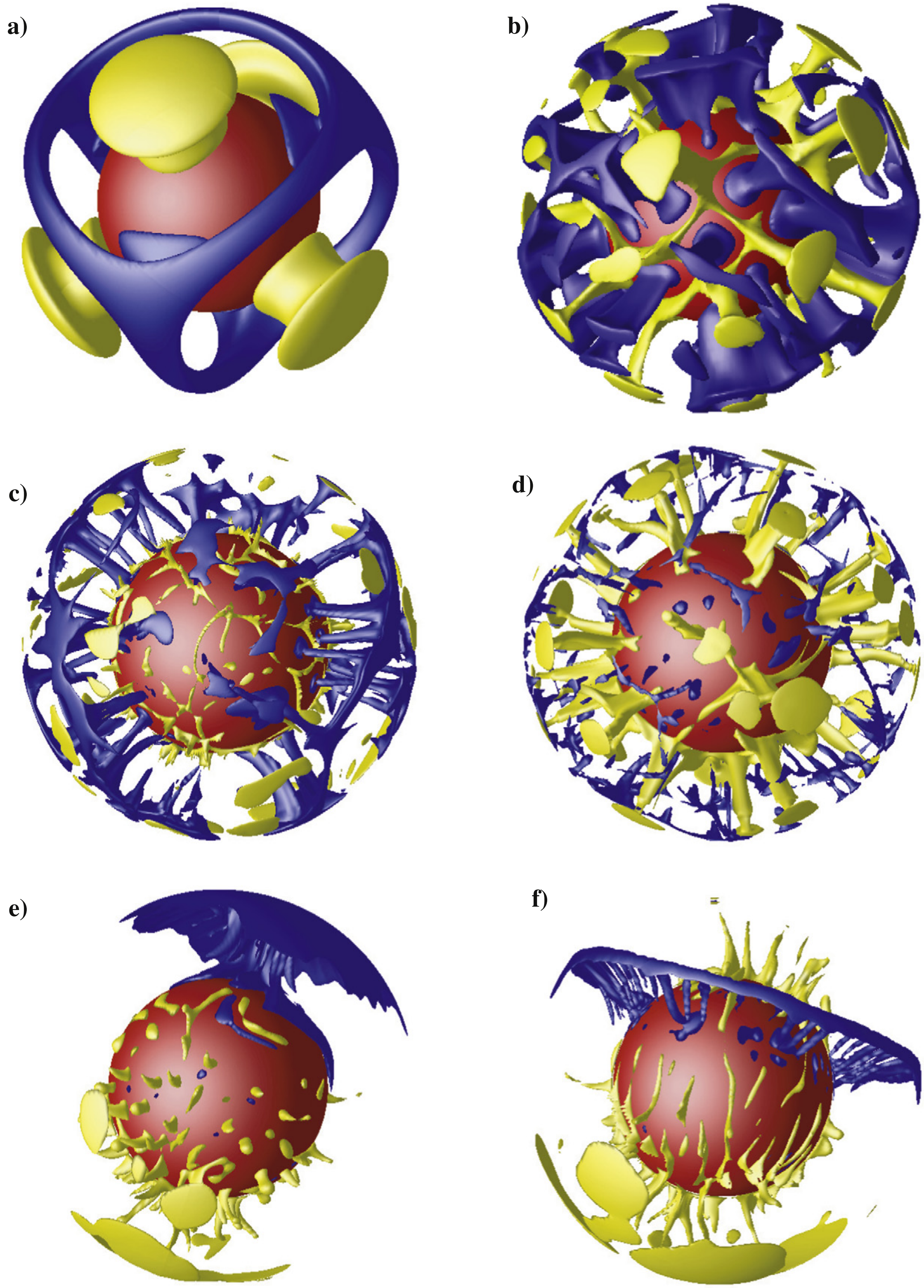

Fig. 6. Convective structures from 3-D fully dynamic models of mantle convection with different model parameters. (a) isoviscous, basal heating convection at Ra = $7x10^3$ with stable tetrahedral convective structure, b) isoviscous, mixed heating (60% internal heating) convection at Ra = $2.43x10^5$, c) mixed heating convection (50% internal heating) with temperature-dependent viscosity (10^3 viscosity variations for non-dimensional temperature changing from 0 to 1) at Ra = $4.56x10^6$, d) the same convection model as in Fig. 6c but with a factor of 30 viscosity reduction for the top 670 km, e) the same convection model as in Fig. 6d but with increased lithospheric viscosity, showing degree-1 convection, and f) the same convection model as in Fig. 6e but with an imposed supercontinent at the surface, showing degree-2 convection with two-antipodal upwellings, one of which is beneath the supercontinent. Fig. 6a, b, and c-e were modified from Zhong et al. (2008), Zhong et al. (2000a), and Zhong et al. (2007), respectively. The yellow and blue isosurfaces of residual temperature represent hot upwellings and cold downwellings, respectively.

(Christensen and Yuen, 1985; Tackley, 1996a). Recent studies of seismology suggest that the Clapeyron slope is probably ~ -2.5 MPa/K (e.g., Fukao et al., 2009), and mineral physics experiments indicate that the Claypeyron slopes for ringwoodite or postspinel phase change range from -0.5 to -2.0 MPa/K (e.g., Fei et al., 2004; Litasov et al., 2005). These values are significantly smaller than that used in the previous convection studies (e.g., Tackley et al., 1993; Tackley, 1996a). Additionally, the role of the phase change in mantle dynamics is significantly weakened by temperature-dependent viscosity that would enhance slab penetration into the lower mantle (e.g., Zhong and Gurnis, 1994) but were not considered in the previous convection studies (e.g., Tackley et al., 1993).

Thermal convection with temperature-dependent viscosity in mobile-lid convection regime has larger convective wavelengths relative to that with uniform viscosity at moderate Ra in 3-D Cartesian (Tackley, 1993) and spherical models (Ratcliff et al., 1997; Zhong et al., 2000a, 2007) (Fig. 6c). The increased convective wavelengths may be mostly due to the depth-dependence of viscosity resulting from the temperature-dependence (e.g., strong top and weak bottom thermal boundary layers due to the temperature effect) (Tackley, 1996b). By adjusting activation energy and internal heating ratio, different depth-dependent temperature and viscosity profiles may be obtained, and some viscosity profiles may lead to predominantly degree-1 convection at modest Ra – the longest wavelength for a spherical geometry (McNamara and Zhong, 2005b; Yoshida and Kageyama, 2006). The main controlling parameter for generating long-wavelength convection is the viscosity contrast between the lithosphere and its underlying mantle, and when this viscosity contrast is between 200 and 10^3, predominantly degree-1 and -2 convection may occur (McNamara and Zhong, 2005b). A similar conclusion was also reached in studies of Martian mantle convection using depth-dependent viscosity (i.e., 1-D viscosity) (Harder, 2000). However, at relatively large Ra (but still smaller than the Earth's Ra), the dominant convective wavelengths reduce to degree 5 to 6, insufficient to explain the observed degree-2 mantle structure (McNamara and Zhong, 2005b).

It was also suggested that an increase in mantle viscosity of a factor of 30 from the upper to lower mantles, as inferred from the geoid studies (Hager and Richards, 1989), would also lead to increased convective wavelengths relative to uniform viscosity models, but the dominant wavelengths were found at degrees 5-8 for convection at modest Ra and with depth-dependent (i.e., 1-D) viscosity but without lithosphere (Bunge et al., 1996). However, it was found that the viscosity increase at the 670 km depth was not efficient in increasing convective wavelengths as Rayleigh number increases (Tackley, 1996a). Indeed, the dominant convective wavelengths in convection with a factor of 30 viscosity increase in the lower mantle and moderately temperature-dependent viscosity (Fig. 6d) are even smaller than that from convection with the temperature-dependent viscosity alone (Fig. 6c) (Zhong et al., 2000a, 2007).

Zhong et al. (2007) found that the most robust way to produce long-wavelength convective structures (e.g., degree-1 or 2) would be to combine both a moderately strong top thermal boundary layer (i.e., lithosphere) and a viscosity increase of a factor of 30 at the 670 km depth. Predominantly degree-1 convection may be generated using this type of viscosity structure with lithospheric viscosity that is about >100 times stronger than the upper mantle (but not so strong to cause stagnant-lid convection (Moresi and Solomatov, 1995), independent of Ra (i.e., at least up to the Earth-type of Ra), heating mode and initial conditions (Fig. 6e) (Zhong et al., 2007). The required viscosity contrasts between the lithosphere and upper mantle and across the 670 km depth for producing these long-wavelength structures are broadly consistent with those inferred from the geoid (e.g., Hager and Richards, 1989) and lithospheric dynamics (England and Molnar, 1997; Flesch et al., 2000). By adjusting these viscosity contrasts, mantle convection of vastly different wavelengths (i.e., from degree-1 to degree-10) can be robustly generated (Liu and Zhong, 2014) (Fig. 7).

3.3. A broad view on long-wavelength structure from fully dynamic models

It should be pointed out that predominantly degree-1 mantle convection may be relevant to dynamic processes in other planetary bodies in the solar system including the Moon, Mars and Enceladus, because they display degree-1 or hemispherically asymmetric features on the surface. These features include the crustal dichotomy and Tharsis volcanism on Mars (e.g., Zuber, 2001), and global asymmetries in mare basalts (i.e., on the nearside) on the Moon (e.g., Wieczorek et al., 2006) and re-surfacing and deformation (i.e., on the southern hemisphere) of Enceladus (e.g., Spencer and Nimmo, 2013). The radially stratified viscosity structure may lead to degree-1 stagnant-lid mantle convection that may help explain the crustal dichotomy and Tharsis Rise on Mars (Zhong and Zuber, 2001; Ke and Solomatov, 2006; Roberts and Zhong, 2006; Zhong, 2009), and radially stratified viscosity or a small metallic core may explain the global asymmetry of the lunar mare basalts (e.g., Zhong et al., 2000b; Parmentier et al., 2002). Although the present-day Earth's mantle structure is predominately degree-2 as discussed earlier, degree-1 convection may be relevant in early geological time, for example, for supercontinent Pangea formation (Zhong et al., 2007), as to be discussed later.

Although the numerical models demonstrate the effect of radially stratified viscosity structure on convective wavelengths (Figs. 6c-e and 7), it remains a challenge to understand the underlying physics of the modeling results. Three types of analyses may be helpful in understanding formation of convective structures. First, a classical linear stability analysis is sometimes used to infer dominant convective wavelengths. For 2-D basal heating convection in an isoviscous fluid with free-slip boundary conditions, critical Ra is the smallest when the horizontal and vertical dimensions of convection are about the same, suggesting that the preferred convective wavelength is about twice of the depth of the flow (Turcotte and Schubert, 2002). However, similar linear stability analyses for convection with two-layer viscosity structure showed that convection would be confined in the weaker layer with reduced horizontal scales of convection when the weak layer is sufficiently weak (e.g., by a factor of ~70) relative to the strong layer (Buffett et al., 1994). This suggests that the effect of radial stratified viscosity on convective structures for large Ra convection may not be explained by the linear stability analyses. This may be because the linear stability analyses are valid only for convection at Ra near critical Ra.

The second approach is based on the premise that a preferred convective wavelength is such that leads to the most efficient heat transfer (e.g., Turcotte and Schubert, 2002). For 2-D basal heating convection in an isoviscous fluid with free-slip boundary conditions, the efficiency of heat transfer or Nusselt number, Nu, can be determined from a boundary layer theory, and the preferred convective wavelength that maximizes Nu is twice of the depth of the flow, similar to that from the linear stability analysis (Turcotte and Schubert, 2002). A boundary layer theory analysis for 2-D convection with vertically stratified viscosity (Busse et al., 2006; Lenardic et al., 2006) found that the preferred wavelength (i.e., the wavelength that maximizes Nu) would scale with the viscosity contrast between the strong and weak layers to 1/4 exponent. This scaling relation is consistent with 2-D thermal convection at different Ra from numerical models (Lenardic et al., 2006). The 2-D numerical models of Lenardic et al. (2006) also showed that a moderately strong lithosphere would promote long-wavelength mantle convection for internally heated convection, consistent with 3-D spherical models of mantle convection discussed earlier (McNamara and Zhong, 2005b; Zhong et al., 2007). Lenardic et al. (2006) proposed that the weak layer would reduce lateral dissipation, which is the key to increased convective wavelength and more efficient heat transfer. This work has been expanded further by Hoeink and Lenardic (2008) in 3-D convection models.

While the analyses by Lenardic et al. (2006) are appealing, some cautionary notes are warranted here. To determine preferred convective wavelengths by maximizing heat transfer has always been controversial in fluid dynamics (e.g., Koschmieder, 1993). Indeed, different stable convective planform could exist with different wavelengths and heat flux in models of the same parameters including viscosity structure and Ra, as shown in Lenardic et al. (2006), suggesting that convective wavelengths are not necessarily associated with the most efficient heat transfer. 2-D convection models showed that convection with larger wavelengths would have smaller heat flux (Zhong and Gurnis, 1994; Grigne et al., 2005), which again seems to suggest a complicated relation between heat transfer and convective wavelengths. It is also unclear why reduced lateral dissipation would lead to longer convective wavelength and more efficient heat transfer, considering that the total dissipation of convection is linearly proportional to surface heat flux with a larger dissipation leading to higher surface heat flux (Hewitt et al., 1975; Jarvis and McKenzie, 1980).

The third approach to determining preferred convective wavelengths is to consider a simple Rayleigh-Taylor instability analysis (e.g., Ribe and de Valpine, 1994; Conrad and Molnar, 1997; Turcotte and Schubert, 2002). Typically, a two-layer model is formulated with the top layer of a larger density overlying the bottom layer of a smaller density (i.e., gravitationally unstable) to determine the growth rates of instability at different wavelengths (Fig. 8a). A preferred wavelength is that with the fastest growth rate of the instability (Turcotte and Schubert, 2002). Rayleigh-Taylor instability analyses were performed in models of a spherical geometry to determine the preferred wavelengths for different viscosity contrast between the top and bottom layers, η_t/η_b (where η_t and η_b are the viscosities for the top and bottom layers), and radial location of the density interface (Fig. 8a) (Zhong et al., 2000b; Zhong and Zuber, 2001). When the two layers have the same viscosity ($\eta_t = \eta_b$), the longest preferred wavelength is at spherical harmonic degree 5 when the two layers have similar thickness (i.e., the density interface is at the mid-mantle depths), but the preferred wavelengths are shorter when either the top or bottom layer gets thinner (Fig. 8b). The preferred wavelengths increase for radially stratified viscosity structure with either $\eta_t > \eta_b$ or $\eta_t < \eta_b$. The preferred wavelengths could get to degree-1 and -2, when a relatively thin top layer is >~100's times more viscous than the bottom layer or when the top layer is 100's times weaker than the bottom layer (Fig. 8b). Although the Rayleigh-Taylor analysis did not consider the energy conservation equation, the predicted preferred wavelengths explain well the predominant convective structure and wavelengths from 3-D mantle convection models, for example, how a moderately strong lithosphere (McNamara and Zhong, 2005b; Zhong et al., 2007) or a weak upper mantle would lead to degree-1 or -2 convection (Ke and Solomatov, 2006; Roberts and Zhong, 2006; Zhong et al., 2007; Sramek and Zhong, 2010).

In summary, it seems that all these three approaches have potential drawbacks in explaining convective structures from 3-D spherical models of mantle convection at large Ra, which would require more studies to illuminate the controlling physical process beyond what have been done so far (Buffett et al., 1994; Zhong and Zuber, 2001; Lenardic et al., 2006).

A final remark is on the lithospheric viscosity. The mobile-lid convection models suggested an important role of lithospheric viscosity in generating very long-wavelength mantle convection (Figs. 6e and 7) (e.g., Zhong et al., 2007). Lithospheric deformation in plate tectonic type of convection occurs mainly at plate boundaries via faulting and yielding (e.g., Bercovici, 2003). However, the mobile-lid convection models presented here (Fig. 6e) did not consider any faulting and yielding deformation mechanisms. Therefore, the lithospheric viscosity in these mobile-lid convection models represents an averaged effective viscosity of plate boundaries. Some attempts have been made to account for these plate boundary processes or their proxies in mantle convection calculations (e.g., Moresi and Solomatov, 1998; Zhong et al., 1998; Richards et al., 2001; Tackley, 2000; Bercovici, 2003; Foley and Becker, 2009; Yoshida and Santosh, 2011; Bercovici and Ricard, 2014). However, lithospheric deformation and rheology is highly non-linear and complicated and significant progress in mantle and lithospheric

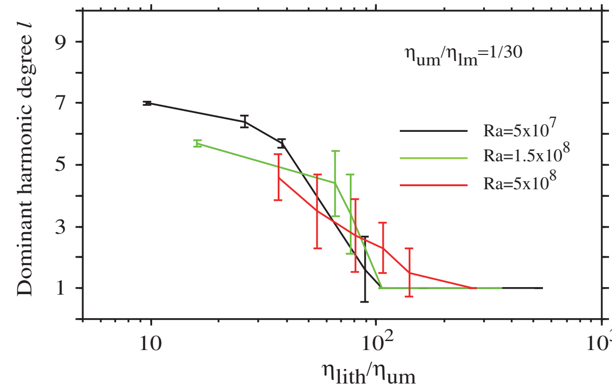

Fig. 7. Dominant spherical harmonic degree l (i.e., convective wavelength) of convective structure versus the ratio of lithospheric to upper mantle viscosities η_{lith}/η_{um} from 3-D fully dynamic models of thermal convection with temperature- and depth-dependent viscosity (Liu and Zhong, 2014). The models are similar to those in Zhong et al. (2007) (e.g., Fig. 6c-e) but with a larger range of model parameters of Rayleigh number Ra and η_{lith}/η_{um}. For all the calculations, the upper mantle is 30 times weaker than the lower mantle (i.e., $\eta_{um}/\eta_{lm} = 1/30$), and temperature-dependent viscosity gives rise to 10^3 viscosity variations for dimensionless temperature varying from 0 to 1. The spectral analyses are done for quasi-steady state temperature field at 100 km above the CMB, and the dominant harmonic degree l is the averaged over some time period.

dynamics may require multi-disciplinary approach to lithospheric rheology involving laboratory (Warren and Hirth, 2006; Mei et al., 2010), modeling in-situ observations (e.g., Zhong and Watts, 2013) and theoretical studies (Bercovici and Ricard, 2012).

4. Long-wavelength Mantle Structures in the Geological Past

Given that the present-day Earth's mantle structure is predominantly at degree-2, an intriguing question is what the mantle structure has been in the past. A large number of studies on thermal evolution of the Earth's mantle have been done in the past but mostly on mantle potential temperature in parameterized mantle convection models (e.g., Davies, 1993; Korenaga, 2008). Although 3-D convection models display significant time-dependent dynamics at modest to large Ra (e.g., Bercovici et al., 1989a; Tackley et al., 1993; Bunge et al., 1998; McNamara and Zhong, 2005a), these models have largely focused on understanding the present-day Earth's mantle structure (i.e., the degree-2). However, increasingly more observations have been made about the temporal and spatial patterns in tectonics and volcanism, and have started to shed light on the possible scenarios of time-evolution of mantle dynamics and structure. Despite significant challenges in integrating relevant observations and dynamics together, two contrasting proposals for temporal evolution of mantle structure in the last 500 Ma have been proposed in recent years (Torsvik et al., 2006; Zhong et al., 2007; Torsvik et al., 2010; Zhang et al., 2010; Torsvik et al., 2014).

4.1. Observational Constraints and Previous Studies

The most robust and significant observational constraint on the Earth's dynamic history is probably the formation and breakup of supercontinents Pangea and Rodinia in the last billion years (e.g., Evans, 2003; Li and Zhong, 2009). Given the established relation between the present-day mantle structure and plate tectonic motions in the last 120 Ma (e.g., Bunge et al., 1998; McNamara and Zhong, 2005a), it is expected that supercontinent assembly and breakup processes would be associated with mantle dynamics and structure. Other observations that may also have implications for temporal evolution of mantle structure and dynamics include true polar wander (TPW), continental flooding, global sea-level changes, and magnetic polarity reversal frequencies, as to be reviewed.

According to Hoffman (1991) and Scotese (1997), the assembly of Pangea was completed by ~330 Ma in the Carboniferous as Gondwana and Laurussia collided near the equator (Fig. 9a), while the breakup of Pangea started at ~175 Ma in the Middle Jurassic, first with North America breaking away from Africa, South America and Eurasia, followed with a sequence of breakups from ~140 Ma to 100 Ma in the Cretaceous between Antarctic, Australia, Africa and South America. The formation of Pangea and the collisions among continental blocks generated mountain belts including Appalachians and Urals, and the Pangea's breakup led to formation of major oceans including Atlantic Ocean. It has also been well accepted in geological community that supercontinent Rodinia may have formed at ~900 Ma and broken up at ~750 Ma (Fig. 9b) (e.g., Torsvik, 2003; Li et al., 2008), suggesting possibly a cyclic process for supercontinents. There are a number of general characteristics of Pangea and Rodinia supercontinent processes. Magmatism and volcanism recorded on continents appeared to have peaked during the breakup of Pangea and Rodinia, while at a minimal level during their formation periods (Fig. 9c-d) (e.g., Ernst and Bleeker, 2010; Torsvik et al., 2010). Both Pangea and Rodinia appeared to have been largely surrounded by subduction zones during and after their formation (Fig. 9a-b). Major subduction zones may have also existed between major continental blocks before they collided to form supercontinents. Both Pangea and Rodinia seemed to have existed only for ~150 Ma before their breakups, while the whole assembly and breakup process may have taken ~500-600 Ma (e.g., Evans, 2003).

True polar wander (TPW) represents the migration of the Earth's spin axis as a result of the change of the Earth's dynamic moment of inertia (e.g., Goldreich and Toomre, 1969). As the Earth's dynamic moment of inertia is controlled by degree-2 non-hydrostatic geoid anomalies, TPW may provide constraints on the Earth's mantle structure. However, it is challenging to infer TPW in the Earth's history, because one must seek for coherent motion of all tectonic and continental blocks over a geological time period from often scarce paleomagnetic observations that do not constrain longitudes of continental blocks (e.g., Besse and Courtillot, 2002; Evans, 2003; Maloof et al., 2006). TPW for the last 200 Ma appeared to be episodic and amounted to ~30 degrees in total (Besse and Courtillot, 2002). However, some significant TPW events have been inferred for earlier time periods (van der Voo, 1994; Maloof et al., 2006). In a recent model for the last 520 Ma plate motion history, 10 TPW events were included with constraints on their polar wander paths (Torsvik et al., 2014).

Large-scale continental flooding and global sea-level changes occurred repeatedly in Phanerozoic, for example, from the early to middle Paleozoic, and from the late Mesozoic to early Cenozoic (Hallam, 1984). The continental flooding has been attributed to the effects of averaged seafloor age (Flemming and Roberts, 1973; Pitman, 1978) and dynamic topography caused by subducted slabs (Mitrovica et al., 1989; Gurnis, 1993). Subducted slabs with their negative buoyancy may cause surface depression (e.g., Hager and Richards, 1989). Subduction history from paleogeographic reconstruction models has been used to construct dynamic models of mantle flow driven by the slabs' negative buoyancy to predict dynamic topography, the sea-level change and continental flooding (Gurnis, 1993). Averaged seafloor age affects global sea-level because of its effect on seafloor topography. The younger the averaged seafloor is, the shallower the ocean basins are and the higher the global sea level is. Averaged seafloor age is determined by seafloor spreading rate and size distribution of tectonic plates (Kominz, 1984; Loyd et al., 2007). Therefore, global sea level change and continental flooding may help constrain mantle dynamic history.

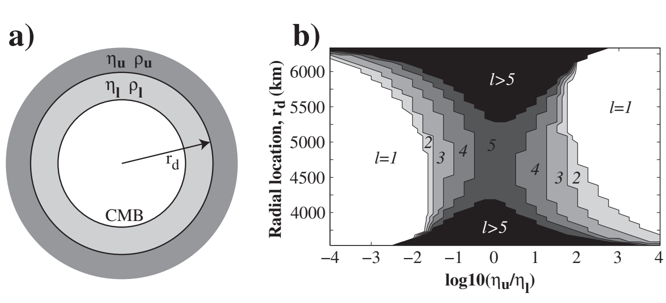

Fig. 8. The setup of a Rayleigh-Taylor instability analysis in spherical geometry using an analytical model by Zhong and Zuber (2001)(a), and preferred wavelengths (i.e., spherical harmonic degree, l) predicted from the Rayleigh-Taylor instability analysis for different viscosity contrasts between the top and bottom layers, η_t/η_b, and different radial location of the density interface (b). The results show that radially stratified viscosity leads to long-wavelength structure.

The Earth's magnetic polarity reversals occurred at highly variable frequencies from several reversals per million years in the most recent history to once every tens of millions of years (e.g., the Cretaceous and Permian superchrons) (Ogg, 2012). While the dynamics of magnetic polarity reversals is still not well understood, the CMB heat flux pattern is believed to play a major role (e.g., Glatzmaier et al., 1999; Olson et al., 2010). Therefore, the observed vastly different polarity reversal frequencies may imply significant temporal variations in the patterns of CMB heat flux and hence mantle structures (Olson et al., 2010).

4.2. A Scenario with a Spatially Stable Degree-2 Mantle Structure

Torsvik et al. (2010, 2014) proposed that the Earth's mantle may have had a predominantly degree-2 structure that is similar to the present-day's mantle with African and Pacific LLSVPs for the last 500 Ma. This proposal was mainly based on correlation of eruption sites of LIPs with the edges of LLSVPs (Fig. 3b) (Torsvik et al., 2006). As discussed in Section 2.4, the hotspots, if projected vertically down to the CMB, were found to preferentially locate in the African and Pacific LLSVPs (e.g., Hager et al., 1985) or in the regions with large horizontal gradients in S-wave models (i.e., mostly near the boundaries of LLSVPs) (Thorne et al., 2004). Torsvik et al. (2006) showed that the original eruption sites of LIPs in the last 200 Ma, after they were restored using the plate motion history model, would be approximately also above the edges of LLSVPs which the authors defined as the 1% contour of S-wave velocity anomalies near the CMB in the Smean model (Fig. 3b) (Becker and Boschi, 2002). This spatial correlation led Torsvik et al. (2006) to propose that the two LLSVPs have remained in the mantle fixed for the last 200 Ma. Subsequently, Torsvik and his colleagues, by considering older LIPs (Torsvik et al., 2008a,b) and kimberlites, suggested that the LLSVPs have been spatially stationary for the last 320 Ma (Torsvik et al., 2010). By analyzing the quadrupole component (i.e., degree-2 poloidal field) of plate motions of the last 250 Ma, Conrad et al. (2013) concluded that the two major upwelling systems associated with the LLSVPs have been stationary for the last 250 Ma, although Rudolph and Zhong (2013) showed that the degree-2 poloidal field of plate motions alone would not be representative of the overall plate divergence.

More significantly, on the basis of the proposed stationary LLSVPs and eruption of LIPs at the edges of LLSVPs, Torsvik et al (2014) and Domeier and Torsvik (2014) reconstructed paleogeography, continental motions and global plate motions for the Paleozoic (i.e., from 540 to 250 Ma), using an iterative scheme that would determine the locations of continental blocks and TPW events and minimize the impact of the longitude ambiguity in paleomagnetic studies. Different from previous studies on reconstructions of paleogeography (e.g., Scotese, 1997) and of global plate motion history (e.g., Gordon and Jurdy, 1986), the reconstruction scheme by Torsvik et al. (2014) and Domeier and Torsvik (2014) placed an important role on the African and Pacific LLSVPs. First, in modeling the TPW events (10 events in total), the Earth's spin axis was constrained to follow a great circle path such that the African and Pacific LLSVPs were always in the equatorial regions and antipodal to each other. This great circle path for the spin axis would follow the negative degree-2 geoid anomalies for the present-day Earth and would have an axis at 0°N and 11°E going through the centers of two LLSVPs (Fig. 3a). In practice, a coherent rotational motion for all the continental blocks was determined first, but only its projected component onto the (0°N, 11°E) axis was considered as possible TPW motion. Second, while the latitudes of a continental block was constrained by paleomagnetic data, its longitudes, whenever possible, was constrained by placing relevant LIPs and kimberlites from the continent at the edges of either African or Pacific LLSVPs. The scheme invoked an iterative approach to make use of the above-mentioned rules and geological data to finally come up with the paleogeography and continental motions for the Paleozoic as summarized in Torsvik et al. (2014).

The spatial correlation of LIP eruptions with the edges of the African and Pacific LLSVPs for the last 200 Ma (Torsvik et al., 2006) provided appealing observational constraints on when the present-day degree-2 mantle structure including the LLSVPs may have been formed. However, given the significance and potential impact of the proposals that the African and Pacific LLSVPs have been stationary for the last 540 Ma and that the LIPs and kimberlites over this time period have erupted at the edges of stationary LLSVPs, it is important to scrutinize the relevant arguments and evidence.

First, the role of the LIPs older than 200 Ma as evidence in supporting the stationary LLSVPs beyond 200 Ma deserves some discussion. Although there were ~20 LIPs since the breakup of Pangea for the last 200 Ma, only five LIPs were identified between 200 Ma and 520 Ma: Siberian Traps at ~250 Ma, Emeishan at ~258 Ma, Skagerrak at ~297 Ma, Yakutsk at ~360 Ma, and Kalkarindji at ~510 Ma (Torsvik et al., 2008a) (Figs. 3b and 9d). This is consistent with active magmatism and volcanism during supercontinent breakup (Fig. 9c) (Ernst and Bleeker, 2010). It was recognized in Torsvik et al (2006) that Siberian Traps fit to neither the African nor Pacific LLSVPs. The eruption locations of other four Paleozoic LIPs and their host continental blocks were generally poorly constrained by paleomagnetic and geological data. Torsvik et al. (2008a,b) decided to place the eruption locations of these four LIPs at the edges of either African or Pacific LLSVPs, assuming that the empirical spatial relation between the LLSVPs and LIPs for the last 200 Ma holds as well for earlier time periods. For example, in placing Emeishan LIP at the western edge of the Pacific LLSVP, Torsvik et al. (2008a) stated in their Fig. 5's caption that "… *Because South China was not part of Pangea, its longitudinal relation to South Africa is unknown and, on palaeomagnetic evidence, it can be placed anywhere in palaeolongitude but not adjacent to Pangea and the African LLSVP. However, if the 258 Ma Emeishan LIP was erupted from a plume derived from the 1% slow shear wave velocity contour in the lowermost mantle of one of the Earth's two major LLSVP's, the only likely position would be along the western edge of the Pacific LLSVP*". Therefore, it seems that these >250 Ma LIPs at the edges of the LLSVPs in Torsvik et al. (2010, 2014) were consequence of the assumption of rather than evidence for stationary African and Pacific LLSVPs during those times. It is unclear whether such determined locations of LIPs and continental blocks in Paleozoic relative to the LLSVPs may have affected the correlation of kimberlites with the LLSVPs in Torsvik et al. (2010, 2014). Also notice that significant number of kimberlites (e.g., in Canada and China) were excluded in the correlation studies of Torsvik et al. (2010).

Second, while proposed LIP eruptions at the edges of thermochemical piles in Torsvik et al (2006) are supported by mantle dynamic models (Tan et al., 2011), the 20 LIPs in the last 200 Ma do not necessarily support the proposed fixity of the LLSVPs for the last 200 Ma. This is because these LIPs erupted at different times, and for the last 200 Ma

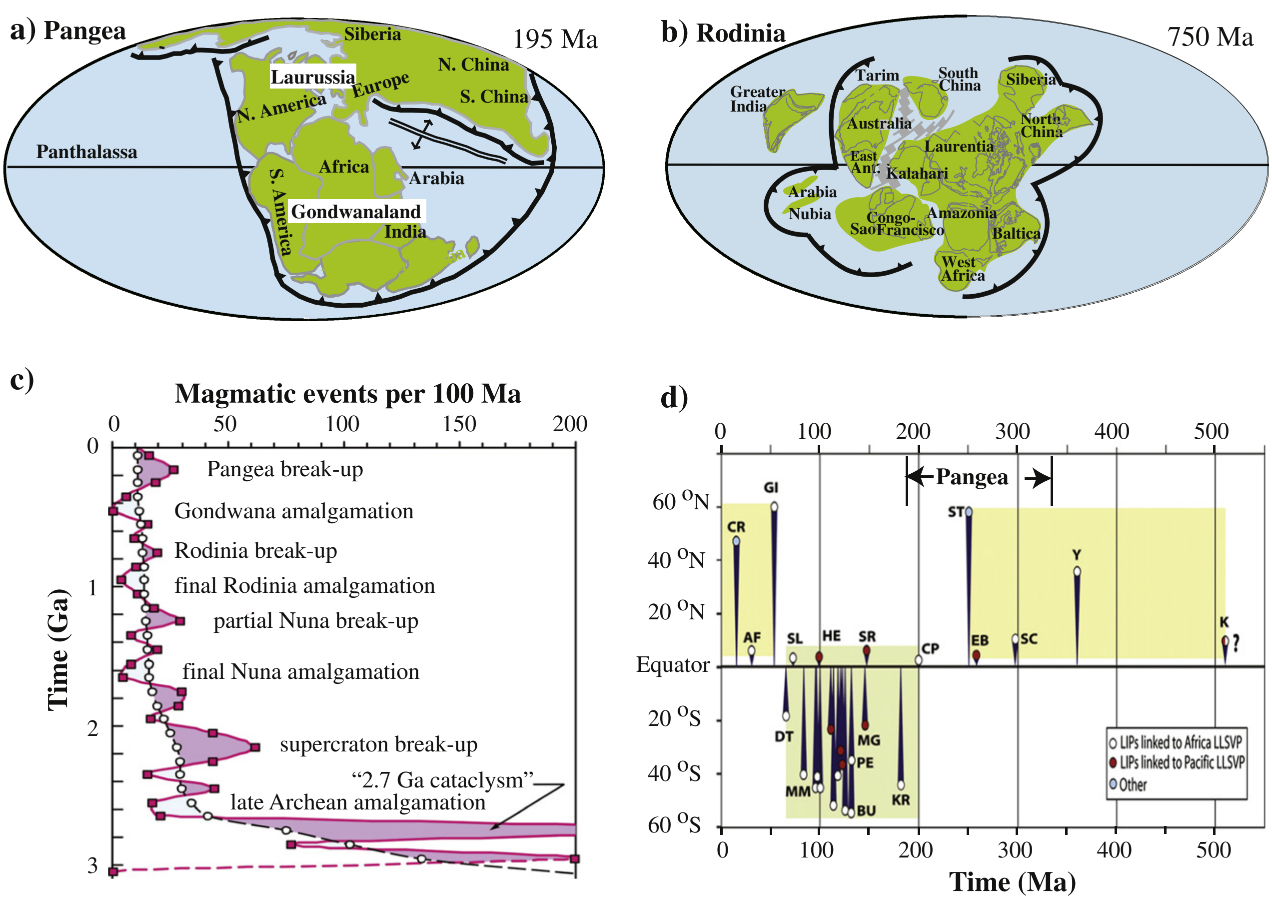

Fig. 9. Supercontinents Pangea at 195 Ma (Scotese, 1997) (a) and Rodinia at 750 Ma (Li et al., 2008) (b), time-dependent magmatism for the last 2.7 Ga (Ernst and Bleeker, 2010) (c), and time-dependent LIP events for the last 500 Ma (Torsvik et al., 2008a). Fig. 9a-b, c, and d were modified from Zhong et al. (2007), Ernst and Bleeker (2010), and Torsvik et al. (2008a), respectively. In Fig. 9c, the magmatic events represent secular pulses of short-lived mafic magmatic events binned per 100 Myrs. In Fig. 9d, each symbol with abbreviation represents a LIP event (see Torsvik et al. (2008a) for details of abbreviation), and the latitudes of LIP eruptions were also given.

there was on average only one LIP event per 10 Myrs (Fig. 9d), which is not sufficient to define as complicated boundaries as the two LLSVPs (Fig. 3b). Clearly, the LIPs in the Paleozoic do not provide the necessary support for the proposed fixity of the LLSVPs, as discussed in the last paragraph. A couple of recent studies have also debated the statistical significance of the LIPs erupting at the edges of the LLSVPs (Austermann et al., 2014; Davies et al., 2015). Furthermore, while dynamic models predicted that many plumes would generate and rise along the edges of chemical piles, a significant fraction of mantle plumes would also not be associated with the chemical piles (Tan et al., 2011). Mantle plumes may tilt significantly during their ascent due to global mantle flow (Steinberger and O'Connell, 2000; Zhong et al., 2000a; Boschi et al., 2007).

Third, TPW was a distinct feature in the reconstructions of paleogeography and plate motions in Torsvik et al. (2014) and Domeier and Torsvik (2014), but the robustness of the inferred TPW could be questionable because of the assumption of stationary present-day degree-2 geoid associated with the African and Pacific LLSVPs. The proposed fixity of the African and Pacific LLSVPs near the CMB is not strongly supported by the observations beyond 200 Ma as discussed earlier, therefore there is no strong basis to use the present-day geoid associated with the LLSVPs to constrain the TPW path in the Paleozoic. Even if the LLSVPs had been relatively stationary near the CMB as possibly for the last 200 Ma, caution would also be needed in using the present-day geoid to constrain the TPW path. TWP is controlled by degree-2 geoid anomalies that are sensitive to the buoyancy and viscosity throughout the mantle, particularly in the mantle transition zones and the middle mantle (e.g., Hager and Richards, 1989). Also, downwellings are likely to play a significant role in controlling the TPW (Richards et al., 1997; Steinberger and Torsvik, 2008). If the two LLSVPs represent thermochemical anomalies as having been hypothesized (e.g., McNamara and Zhong, 2005a), the long-wavelength geoid anomalies would be controlled by mantle structure in the top 1700 km of the mantle, and the bottom 1000 km of the mantle including the LLSVPs would not have any net contribution to the geoid (Liu and Zhong, 2014, 2015). It should also be pointed out that the TPW, if determined incorrectly, would introduce spurious lithospheric net rotation in plate motion models, causing dynamic inconsistence as discussed recently (Rudolph and Zhong, 2014).

In short, the proposal that the African and Pacific LLSVPs and degree-2 mantle structure may have been relatively stable and stationary for the last 540 Ma by Torsvik et al. (2010, 2014) has potentially important implications for mantle dynamics and paleogeography reconstruction. There is little observational evidence for this proposal beyond 200 Ma. The discussions presented above purposely provided a critical assessment of this proposal with a hope to motivate more vigorous tests of the proposal.

4.3. A Scenario with Alternating Degree-1 and Degree-2 Mantle Structure

Zhong et al. (2007) proposed that the mantle structure was predominantly at degree-1 in the early and middle Paleozoic during and shortly after the Pangea assembly and that the present-day degree-2 mantle structure was formed significantly after Pangea assembly. This model was mainly based on consideration on how a supercontinent may come to form dynamically and what the supercontinent may affect its underlying mantle convection. A degree-1 mantle convection with hot upwellings in one hemisphere and cold downwellings in the other hemisphere would lead continental blocks to collide and merge to a supercontinent in the downwelling hemisphere (e.g., Monin, 1991; Evans, 2003). As discussed in Section 3.2, Zhong et al. (2007) found that degree-1 mantle convection occurs with observationally constrained lithospheric and mantle viscosity structure (Fig. 6e). Such predominantly degree-1 convection would lead to formation of supercontinent on a ~300 Myrs time-scale that is consistent with the inferred for Pangea and Rodinia (Zhang et al., 2009). Once a supercontinent is formed, the circum-supercontinent subduction, as inferred for Pangea and Rodinia (Fig. 9a-b), would lead to upwellings and increased temperature beneath the supercontinent, thus changing the degree-1 mantle structure to degree-2 with two major antipodal upwellings, similar to the present-day Earth's mantle (Fig. 6f) (Zhong et al., 2007). The hot, upwellings beneath the supercontinent would cause magmatism and eventual breakup of the supercontinent.

This model may provide a simple explanation to a number of important observations. The first is the present-day dominantly degree-2 mantle structure with antipodal African and Pacific LLSVPs. The model suggests that the African LLSVP would have been formed after Pangea formation (i.e., after 330 Ma) as a result of upwelling return flow in response to circum-Pangea subduction. This causes the mantle structure to switch from degree-1 to degree-2. The present-day degree-2 mantle structure with two LLSVPs reflects the temporal evolution of mantle convection modulated by Pangea assembly and breakup process (Zhong et al., 2007; Li and Zhong, 2009). This is also consistent with the proposed orthoversion model for supercontinent cycles on the basis of geological considerations (Mitchell et al., 2012). The second is on the temporal variations in magmatism, i.e., reduced level of magmatism between 500 Ma and 200 Ma and enhanced after 180 Ma (Fig. 9c-d) (e.g., Ernst and Bleeker, 2010). During and shortly after Pangea assembly, the mantle in the African hemisphere where the continents were colliding and merging to give rise to mantle downwellings would be relatively cold as predicted from this model (Fig. 6e) (Zhong et al., 2007; Zhang et al., 2009), thus having a reduced magmatism. Once the African upwelling system or LLSVP was formed significantly after the Pangea assembly (Fig. 6f), the magmatism started to increase, followed with the Pangea's breakup (Zhong et al., 2007).

The proposed scenario of mantle structure evolution was confirmed in semi-dynamic models of thermochemical mantle convection with a simple plate motion history model for the last 450 Ma that includes the assembly and breakup processes of Pangea (Zhang et al., 2010). The semi-dynamic model is similar to McNamara and Zhong (2005a) except for using plate motions over longer geological history. The plate motions for the last 120 Ma were taken from Lithgow-Bertelloni and Richards (1998) (Fig. 4a-b) (referred to as LBR1998) that was also used in McNamara and Zhong (2005a). Between 120 Ma and 450 Ma, continental plate motions were determined from paleogeography by Scotese (1997), while the plate motions in the Pacific were assumed to be similar to that at 120 Ma. Given the significant convergence between Laurussia and Gondwana from 450 Ma to 330 Ma in Scotese's paleogeography model (Fig. 4c), subducted slabs were accumulated in the mantle beneath Pangea at 330 Ma in the semi-dynamic model, pushing the thermochemical materials above the CMB away from the African/Pangea hemisphere and leading to a largely degree-1 mantle structure (Fig. 10a) (Zhang et al., 2010). With the circum-Pangea subduction, the African upwelling system and thermochemical pile started to develop, and were largely developed by ~200 Ma (Fig. 10b). The present-day mantle structure from this model (Fig. 10c) is quite similar to the present-day seismic structure (Figs. 1 and 5) (McNamara and Zhong, 2005a; Zhang et al., 2010).

The semi-dynamic model with the plate motion history for the last 450 Ma also makes predictions for temporal evolution of surface dynamic topography and CMB heat flux that have implications for vertical motion history of continental cratons and for core dynamo action (Zhang and Zhong, 2011; Flowers et al., 2012; Zhang et al., 2012; Olson et al., 2013). For example, the model predicts that the Slave craton in North America subsides before Pangea assembly at 330 Ma but uplifts significantly from 330 Ma to 240 Ma in response to pre-Pangea subduction and post-assembly mantle warming (Fig. 11a). The Kaapvaal craton of Africa is predicted to undergo uplift from ~180 Ma to 90Ma after Pangea breakup, but its dynamic topography remains stable for the last 90 Ma (Fig. 11b). These model predictions for the Slave and Kaapvaal cratons compare well with the burial-unroofing histories inferred from thermochronology studies (Fig. 11a-b), thus supporting our dynamic models including the development of the African LLSVP mantle structure (Flowers et al., 2012; Zhang et al., 2012). The predicted CMB heat flux was used in dynamo models to investigate its effects on the polarity reversal frequency and inner core growth history (Olson et al., 2013, 2015). Although the model failed to account for the Cretaceous superchron, it reproduced well other characteristics of polarity reversal frequency (Olson et al., 2013).

4.4. Are the stationary LLSVPs insensitive to surface plate motions?

The general results from the semi-dynamic model of Zhang et al. (2010) are consistent with previous studies (e.g., Hager and O'Connell, 1979; Bunge et al., 1998; McNamara and Zhong, 2005a) in that surface plate motions dictate mantle convection and structure. Particularly, the thermo-chemical piles are passive features that respond to downwellings from above (Tackley, 1998; McNamara and Zhong, 2005a; Tan et al., 2011). The evolution of large-scale mantle structure in these models mostly reflects the plate motion history, that is, the plate motion history of the last ~120-150 Ma for the present-day degree-2 mantle structure (Fig. 10c) and the pre-Pangea plate motions for the degree-1 mantle structure at the Pangea time (Fig. 10a).

Recently, Bull et al. (2014) performed similar semi-dynamic modeling calculations but using different plate motion models: for the Paleozoic (410-250 Ma) (Domeier and Torsvik, 2014) (referred to as DT2014) and the last 200 Ma (Seton et al., 2012) (referred to as S2012). The Paleozoic plate motion model DT2014 was derived by assuming stationary African and Pacific LLSVPs, as discussed in Section 4.2, while the plate motion S2012 was an updated model from Muller et al. (2008). Bull et al. (2014) made three conclusions: 1) The African and Pacific LLSVPs, if used as initial conditions, would have remained close to their present-day positions for at least the last 410 Myr, supporting Torsvik et al. (2010, 2014). 2) The mantle could not have been at dominantly degree-1 structure during the Pangea assembly, because such initial conditions would not have led to the present-day mantle structure. 3) The present-day degree-2 mantle structure with two LLSVPs could not be reproduced using S2012 plate motion for the last 120 Myr, contradicting with McNamara and Zhong (2005a) that used plate motion model LBR1998 (Lithgow-Bertelloni and Richards, 1998).

Zhong and Rudolph (2015) have recently computed a number of models with different plate motion histories including the ones used in Bull et al. (2014), and they obtain the results that are inconsistent with Bull et al. (2014) but confirm the results by McNamara and Zhong (2005a) and Zhang et al. (2010). For example, Zhong and Rudolph (2015) found that using the last 120 Ma plate motion history from either LBR1998 or S2012, the semi-dynamic models would reproduce seismically imaged degree-2 mantle structure including the African and Pacific LLSVPs for the present-day. The models by Zhong and Rudolph (2015), which are similar to those by Zhang et al. (2010), use realistic mantle viscosity inferred from post-glacial rebound studies (e.g., Simons and Hager, 1997; Mitrovica and Forte, 2004) with the lower mantle viscosity of approximately 10^{22} Pas and ~100 times smaller viscosity for the upper mantle. Zhong and Rudolph (2015) found that more viscous lower mantle (i.e., a smaller Rayleigh number) would slow down the development of the lower mantle degree-2 structure. However, using different plate motion history models for the last 250 Ma (e.g., Zhang et al. (2010) or Z2010; DT2014; S2012; LBR1998) and different mantle viscosity, Zhong and Rudolph (2015) conclude that for a reasonable range of mantle viscosity, the present-day lower mantle degree-2 structure is largely caused by plate motion history for the last 150 Ma and may not contain or “remember” significant amount of information before 150 Ma. This result is similar to Bunge et al. (1998) that focused on comparing slab structure using LBR1998 plate motion.

Would the degree-2 structure with the two LLSVPs remain stationary or unchanged for the last 410 Ma using DT2014 plate motion, as suggested in Bull et al. (2014)? Zhong and Rudolph (2015) computed the semi-dynamic convection models using plate motion history for the last 410 Ma (i.e., using DT2014 and S2012) and degree-2 structure with two LLSVPs as initial conditions at 410 Ma, as in Bull et al. (2014). However, Zhong and Rudolph (2015) found that the initially degree-2 lower mantle structure including the shape of the LLSVPs (Fig. 12a) would vary significantly with time before and shortly after Pangea assembly in response to the imposed plate motion history and that the degree-1 structure has grown to be more significant than degree-2 between 350 Ma and 250 Ma (Fig. 12b). After Pangea is formed at ~330 Ma, the circum-Pangea subduction promotes degree-2 structure formation (Zhong et al., 2007; Zhang et al., 2010; Bower et al., 2013). By ~200 Ma, the lower mantle structure is again dominantly degree-2 with the African and Pacific LLSVPs (Fig. 12c) that remain unchanged since. The present-day structure is again dominantly degree-2 with two major LLSVPs and is similar to the initial condition (Fig. 12a and d). Zhong and Rudolph (2015) also conclude that for models with different initial conditions, plate motion history and mantle viscosity, the dominantly degree-2 lower mantle structure with the African and Pacific LLSVPs as observed today may have largely formed the latest by 200 Ma.

It should be pointed out that although the semi-dynamic convection models with DT2014 plate motion also predict significant degree-1 structure in the lower mantle in the early stage of Pangea (e.g., Fig. 12c) (Zhong and Rudolph, 2015), the degree-1 structure is not as strong as that in Zhang et al. (2010) (Fig. 10a). This is expected because the pre-Pangea plate motions in DT2014 included significantly less convergence between Laurussia and Gondwana in forming Pangea than that implied in Scotese's paleogeography reconstruction (see also Torsvik et al. (2014)). However, since the assumptions of the stationary African and Pacific LLSVPs for the last 500 Myrs that were used to build DT2014 are debatable as discussed before, the predicted lower mantle structure at the Pangea time would be subjected to the same debate and may represent one of the possible scenarios, like that from Zhang et al. (2010). The results from Zhong and Rudolph (2015) are in conflict with what have been reported in Bull et al. (2014). It is unclear what have caused the difference. It is possible that Bull et al. (2014) used significantly larger mantle viscosity than that inferred from the observations. It should be pointed out that the plate motion models for Domeier and Torsvik (2014) from 410 Ma to 250 Ma and for Seton et al. (2012) from 200 Ma to the present-day were downloaded from the published websites. However, the plate motions between 250 Ma and 200 Ma are not publically available. Therefore, the plate motions for this 50 Myrs period in Zhong and Rudolph (2015) are likely different in detail from that used in Bull et al. (2014). However, this difference should not affect the conclusion, because the significant time evolution of the lower mantle structure including chemical piles occurs before 250 Ma for which only DT2014 plate motion was relevant (Fig. 12c).

5. Conclusion and future directions

The lower mantle structure of the present-day Earth is characterized by two major seismically slow anomalies beneath Africa and Pacific (i.e., LLSVPs) separated by seismically fast anomalies associated with the past subduction (e.g., Dziewonski, 1984; Ritsema et al., 2011). This structure is often referred as to degree-2 structure. The degree-2 mantle structure has important implications for the Earth's long-wavelength topography, gravity and geoid anomalies, distribution of volcanism, style of mantle convection, and true polar wander. Seismic and geodynamic studies suggest that the LLSVPs are likely chemically distinct from the ambient mantle (Masters et al., 2000; Wen et al., 2001; Ni et al., 2002; McNamara and Zhong, 2005a), although some other studies propose no need for chemical heterogeneity in the LLSVPs (e.g., Schuberth et al., 2009, 2012; Davies et al., 2012). The degree-2 structure in the lower mantle may result from the history of plate tectonic motions and subduction of the last 150 Ma (e.g., Bunge et al., 2002; McNamara and Zhong, 2005a; Zhong and Rudolph, 2015) for mantle viscosity inferred from post-glacial rebound studies. Fully

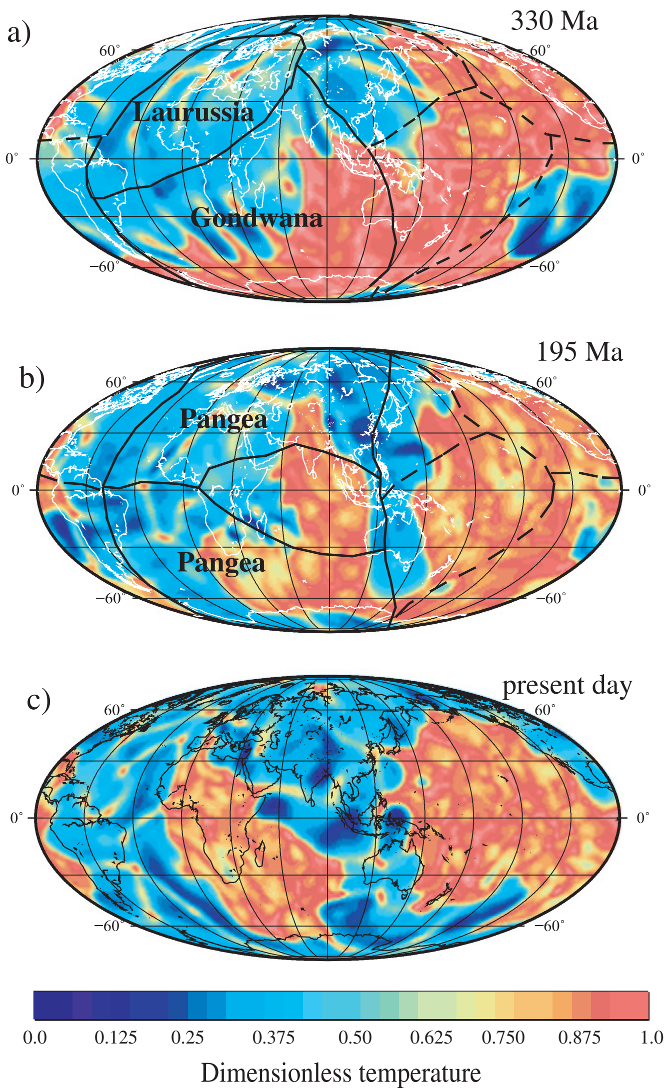

Fig. 10. Mantle thermochemical structure at 2750 km depth from a semi-dynamic convection model by Zhang et al. (2010) at 330 Ma (a), 195 Ma (b), and present-day (c). In these temperature plots, the large regions with high temperature are also where the chemical piles are. The plate motion history model uses plate motions of LBR1998 for the last 120 Ma and continental motions from paleogeography reconstruction of Scotese (1997) for earlier times. The figure was modified from Zhang et al. (2010).

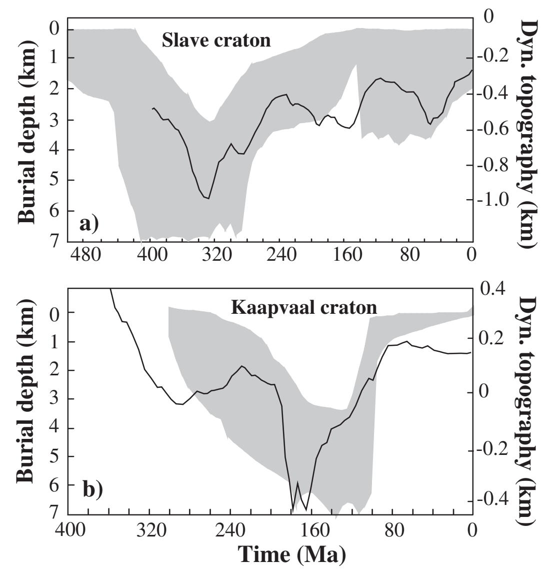

Fig. 11. Predicted time-dependent dynamic topography at the Slave craton (a) and Kaapvaal craton (b) from semi-dynamic convection models of Zhang et al. (2010) (i.e., from Fig. 10) and their comparison with the inferred burial and unroofing history for these two cratons from thermochronology studies (shaded) (Flowers and Schoene, 2010; Flowers et al., 2012). The figure was modified from Zhang et al. (2012).

dynamic models of mantle convection without any imposed surface motions may produce convective structure at wavelengths comparable with the present-day Earth's mantle (i.e., degree-2) at realistic Rayleigh number, using moderately strong lithosphere and lower mantle (Zhong et al., 2007). Even degree-1 mantle convection could be generated with this type of lithospheric and mantle viscosity. The long-wavelength mantle convection may provide a dynamically self-consistent explanation for the present-day mantle structure and large-scale surface tectonics (e.g., Pangea assembly and breakup) and volcanism (Zhong et al., 2007).

The African and Pacific LLSVPs may be the primary source regions for mantle plumes and volcanism including large igneous provinces (LIP) (e.g., Hager et al., 1985; Torsvik et al., 2010), to explain the isotopic heterogeneities in hotspot volcanism (Hofmann, 1997). Hotspot volcanism and LIPs for the last 200 Ma may occur preferentially at the boundaries of the LLSVPs (e.g., Torsvik et al., 2006). While this empirical relation is supported by dynamic models of thermochemical convection (Tan et al., 2011), its statistical significance has also been called into question (Davies et al., 2015; Austermann et al., 2014). However, there is only a very small number of LIPs older than 200 Ma and their eruption sites are poorly constrained by geological and paleomagnetic data (Torsvik et al., 2008a,b). There is no strong evidence for these relatively old LIPs to be associated with the present-day African and Pacific LLSVPs.

While the present-day Earth's mantle structure is dominantly at degree-2, how mantle structure may have evolved in the geological past (e.g., since the early Paleozoic) is an intriguing question that has important implications for time-evolution of volcanism and surface tectonics. The degree-1 mantle convection provides an appealing mechanism for supercontinent formation in the downwelling hemisphere (Zhong et al., 2007). If Pangea was formed in this way, then the mantle in the early Pangea time would have a degree-1 structure, suggesting a transition of degree-1 to degree-2 mantle structure from Pangea to the present-day (Zhong et al., 2007; Zhang et al., 2010). This suggests that the mantle beneath Pangea would experience significant increase in temperature from the early Pangea time to later time, which may be responsible for the Pangea breakup (Gurnis, 1988; Zhong and Gurnis, 1993; Lowman and Jarvis, 1996; Lenardic et al., 2011). These temporal variations in mantle structure and temperature may explain the volcanism history recorded on continents (i.e., a low level of volcanism in the early Pangea time but high before and during Pangea breakup) (Ernst and Bleeker, 2010). The close association of the LIPs of the last 200 Ma with the African and Pacific LLSVPs may suggest that the present-day degree-2 structure may have formed at ~200 Ma (Torsvik et al., 2006), and this appears consistent with the prediction of semi-dynamic models using different plate motion history models and initial conditions (Zhong and Rudolph, 2015).

However, the proposed fixity of the African and Pacific LLSVPs for the last 520 Ma (Torsvik et al., 2010, 2014) lacks robust observational evidence beyond 200 Ma and is not supported by mantle dynamics. Therefore, caution may be exercised in using the fixity for reconstructing paleogeography and constraining locations of continental blocks and true polar wander in the Paleozoic or early Mesozoic (i.e., >200 Ma). The semi-dynamic models using Domeier and Torsvik's (2014) plate motion history for the last 410 Ma derived from the fixity of the African and Pacific LLSVPs predict that the LLSVPs must have moved around significantly in response to the surface plate motions (Zhong and Rudolph, 2015), thus leading to dynamic inconsistency. Generally speaking, it is always possible to construct a global plate motion history model with Pangea assembly and breakup that does not cause significant migration

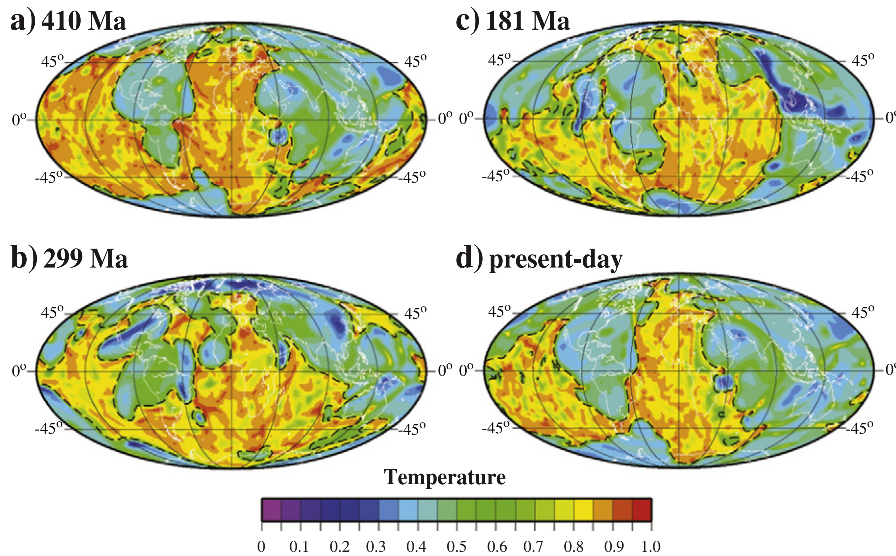

Fig. 12. Time-evolution of thermochemical structures at 2750 km depth from a semi-dynamic mantle convection model of Zhong and Rudolph (2015) using the plate motion history for the last 410 Ma from Domeier and Torsvik (2014) and Seton et al. (2012). Snapshots at 410 Ma or initial condition (a), ~300 Ma (b), ~181 Ma (c), and the present-day (d). The black contour is for composition field C = 0.5. Note that the initial temperature and composition structure in Fig. 12a is taken from the present-day structure from another calculation using Seton et al. (2012) for the last 200 Ma plate motion and that the present-day structure for the current case in Fig. 12d after 410 Myrs time integration becomes nearly identical to the initial condition in Fig. 12a. The calculation shows significant time variations of mantle structure from the initially degree-2 structure at 410 Ma to that with significant degree-1 structure at ~300 Ma using Domeier and Torsvik (2014) plate motion. The figure was taken from Zhong and Rudolph (2015).

of the African and Pacific LLSVPs since the Paleozoic. For example, one can always envision that Pangea was formed above the downwelling regions between the two LLSVPs, and has subsequently moved out of the downwelling region to above the African LLSVP or upwelling. However, even if such a plate motion history model can be built, one must also answer the dynamics question as to why Pangea would move against mantle flow from the downwelling to upwelling regions.

Future studies are needed to further test different hypotheses on the degree-2 mantle structure and the African and Pacific LLSVPs and their time evolution since the early Paleozoic. First, more seismic, mineral physics and geodynamics studies are needed to examine the thermochemical structures in the lower mantle, particularly whether or not and how the LLSVPs are chemically distinct from the bulk of the mantle (Masters et al., 2000; McNamara and Zhong, 2005a; Davies et al., 2012; He and Wen, 2012). Can the anti-correlation between the shear and bulk sound speed anomalies in the lower mantle and LLSVP regions, which is often cited as evidence for chemically distinct LLSVPs, be explained in terms of post-perovskite phase change (Davies et al., 2012)? What are responsible for the significantly different seismic anisotropy in and outside the LLSVPs (Cottaar and Romanowicz, 2013; Lynner and Long, 2014)? If the LLSVPs are chemically distinct, what are the origins of the chemical heterogeneities, primitive or recycled crust or both (e.g., Li et al., 2014; Nakagawa and Tackley, 2014) and how do the chemically distinct and heavy LLSVPs reconcile with the surface geoid anomalies (Liu and Zhong, 2015)? For the latter question, more seismic studies are needed to better resolve mantle structure around ~1800 km depths, as the bottom 1000 km of the mantle including the LLSVPs would be compensated and not produce any net surface geoid (Liu and Zhong, 2015).

Time-evolution of long-wavelength mantle structure is an important topic that requires more observational studies and modeling work to interpret the observations. Improving plate motion history models is important (e.g., Seton et al., 2012), and it is also challenging beyond 200 Ma due to lack of the observations and data in oceanic regions. Observational studies should focus on establishing spatial and temporal patterns of volcanism (e.g., Torsvik et al., 2006; Ernst and Bleeker, 2010) and inferring true polar wandering events, sea-level change and vertical motions of cratons (e.g., Maloof et al., 2006; Ault et al., 2009; Flowers and Schoene, 2010; Flowers et al., 2012). Geochemical observations may also provide important constraints on mantle compositional structure, and hence mantle dynamics (Iwamori and Nakamura, 2015). Through geodynamic modeling, these observations may help constrain time-evolutions of plate motions and of long-wavelength mantle structure (e.g., van Keken and Ballentine, 1999; Zhang et al., 2012; Conrad, 2013; Li et al., 2014).

Finally, there is a need for better understanding the physics behind the long-wavelength convection. While more numerical modeling studies are needed to further examine the role of stratified mantle viscosity, particularly the lithospheric viscosity, in promoting long-wavelength convection (e.g., Zhong et al., 2007), it is equally important to develop an improved understanding both qualitatively and quantitatively about the governing physics of long-wavelength convection (e.g., Lenardic et al., 2006). Given the important role of lithosphere in the dynamics of the mantle and also in relating to observations, incorporating lithosphere in mantle dynamic models is essential. Future geodynamic studies should continue exploring relevant rheological properties of lithosphere (e.g., Arredondo and Billen, 2012; Bercovici and Ricard, 2012; Watts et al., 2013; Zhong and Watts, 2013). At the same time, different forms and approximations of modeling lithosphere including semi-dynamic models with imposed plate motions (e.g., Zhang et al., 2010) and pseudo-plastic rheology in fully dynamic models (e.g., Coltice et al., 2012; Yoshida and Hamano, 2015) should be employed to incorporate lithosphere, continental collision and rifting in global mantle convection models and to integrate and understand geological observations.

Acknowledgement

This work was supported by the National Science Foundation through grant 1135382. CitcomS is available through the Computational Infrastructure for Geodynamics (geodynamics.org). Mr. Chuan Qin helped make Fig. 8 for this paper. The authors would also like to thank W. Leng, Z.X. Li, M.L. Rudolph, and N. Zhang for their contributions to the work presented here, and M. Yoshida and an anonymous reviewer for their constructive reviews.

References

Allegre, C.J., Hofmann, A., O'Nions, K., 1996. The Argon constraints on mantle structure. Geophysical Research Letters 23, 3555–3557. http://dx.doi.org/10.1029/96GL03373.

Allegre, C., Staudacher, T., Sarda, P., Kurz, M., 1983. Constraints on evolution of ##earths mantle from rare-gas systematics. Nature 303, 762–766. http://dx.doi.org/10.1038/303762a0.

Anderson, D., 1982. Hotspots, polar wander, Mesozoic convection and the geoid. Nature 297, 391–393. http://dx.doi.org/10.1038/297391a0.

Arredondo, K.M., Billen, M.I., 2012. Rapid weakening of subducting plates from trench-parallel estimates of flexural rigidity. Physics of the Earth and Planetary Interiors 196, 1–13. http://dx.doi.org/10.1016/j.pepi.2012.02.007.

Ault, A.K., Flowers, R.M., Bowring, S.A., 2009. Phanerozoic burial and unroofing history of the western Slave craton and Wopmay orogen from apatite (U–Th)/He thermochronometry. Earth and Planetary Science Letters 284, 1–11. http://dx.doi.org/10.1016/j.epsl.2009.02.035.

Austermann, J., Kaye, B.T., Mitrovica, J.X., Huybers, P., 2014. A statistical analysis of the correlation between large igneous provinces and lower mantle seismic structure. Geophysical Journal International 197, 1–9. http://dx.doi.org/10.1093/gji/ggt500.

Becker, T.W., 2008. Azimuthal seismic anisotropy constrains net rotation of the lithosphere. Geophysical Research Letters 35, L08308. http://dx.doi.org/10.1029/2008GL033946.

Becker, T.W., 2006. On the effect of temperature and strain-rate dependent viscosity on global mantle flow, net rotation, and plate-driving forces. Geophysical Journal International 167, 943–957. http://dx.doi.org/10.1111/j.1365-246X.2006.03172.x.

Becker, T.W., Boschi, L., 2002. A comparison of tomographic and geodynamic mantle models. Geochemistry, Geophysics, Geosystems 3, 1003. http://dx.doi.org/10.1029/2001GC000168.

Bercovici, D., 2003. The generation of plate tectonics from mantle convection. Earth and Planetary Science Letters 205, 107–121. http://dx.doi.org/10.1016/S0012-821X(02)01009-9.

Bercovici, D., Ricard, Y., 2014. Plate tectonics, damage and inheritance. Nature 508, 513–516. http://dx.doi.org/10.1038/nature13072.

Bercovici, D., Ricard, Y., 2012. Mechanisms for the generation of plate tectonics by two-phase grain-damage and pinning. Physics of the Earth and Planetary Interiors 202, 27–55. http://dx.doi.org/10.1016/j.pepi.2012.05.003.

Bercovici, D., Schubert, G., Glatzmaier, G.A., Zebib, A., 1989a. Three-dimensional thermal convection in a spherical shell. Journal of Fluid Mechanics 206, 75–104.

Bercovici, D., Schubert, G., Glatzmaier, G.A., 1989b. Three-dimensional, spherical models of convection in the Earth's mantle. Science 244, 950–955.

Besse, J., Courtillot, V., 2002. Apparent and true polar wander and the geometry of the geomagnetic field over the last 200 Myr. Journal of Geophysical Research - Solid Earth 107, 2300. http://dx.doi.org/10.1029/2000JB000050.

Boschi, L., Becker, T.W., Steinberger, B., 2007. Mantle plumes: dynamic models and seismic images. Geochemistry, Geophysics, Geosystems 8, Q10006. http://dx.doi.org/10.1029/2007GC001733.

Bower, D.J., Gurnis, M., Seton, M., 2013. Lower mantle structure from paleogeographically constrained dynamic Earth models. Geochemistry, Geophysics, Geosystems 14, 44–63. http://dx.doi.org/10.1029/2012GC004267.

Boyet, M., Carlson, R.W., 2005. Nd-142 evidence for early (>4.53 Ga) global differentiation of the silicate Earth. Science 309, 576–581. http://dx.doi.org/10.1126/science.1113634.

Brune, J.N., Dorman, J., 1963. Seismic waves and earth structure in the Canadian Shield. Bulletin of the Seismological Society of America 53, 167–210.

Buffett, B., Gable, C., Oconnell, R., 1994. Linear-stability of a layered fluid with mobile surface plates. Journal of Geophysical Research - Solid Earth 99, 19885–19900. http://dx.doi.org/10.1029/94JB01556.

Bull, A.L., Domeier, M., Torsvik, T.H., 2014. The effect of plate motion history on the longevity of deep mantle heterogeneities, Earth Planet. Science Letters 401, 172–182.

Bull, A.L., McNamara, A.K., Ritsema, J., 2009. Synthetic tomography of plume clusters and thermochemical piles, Earth Planet. Science Letters 278, 152–162.

Bunge, H.P., 2005. Low plume excess temperature and high core heat flux inferred from non-adiabatic geotherms in internally heated mantle circulation models. Physics of the Earth and Planetary Interiors 153, 3–10. http://dx.doi.org/10.1016/j.pepi.2005.03.017.

Bunge, H.P., Ricard, Y., Matas, J., 2001. Non-adiabaticity in mantle convection. Geophysical Research Letters 28, 879–882.

Bunge, H.P., Richards, M.A., Baumgardner, J.R., 2002. Mantle-circulation models with sequential data assimilation: inferring present-day mantle structure from plate-motion histories. Philosophical Transactions of the Royal Society A: Mathematical, Physical and Engineering Sciences 360, 2545–2567. http://dx.doi.org/10.1098/rsta.2002.1080.

Bunge, H.P., Richards, M.A., Baumgardner, J.R., 1996. Effect of depth-dependent viscosity on the planform of mantle convection. Nature 379, 436–438. http://dx.doi.org/10.1038/379436a0.

Bunge, H.P., Richards, M.A., Lithgow-Bertelloni, C., Baumgardner, J.R., Grand, S.P., Romanowicz, B.A., 1998. Time scales and heterogeneous structure in geodynamic earth models. Science 280, 91–95. http://dx.doi.org/10.1126/science.280.5360.91.

Busse, F.H., Richards, M.A., Lenardic, A., 2006. A simple model of high Prandtl and high Rayleigh number convection bounded by thin low viscosity layers. Geophysical Journal International 164, 160–167. http://dx.doi.org/10.1111/j.1365-246X.2005.02836.x.

Campbell, I., Griffiths, R., 1990. Implications of mantle plume structure for the evolution of flood basalts. Earth and Planetary Science Letters 99, 79–93. http://dx.doi.org/10.1016/0012-821X(90)90072-6.

Castle, J.C., Van der Hilst, R.D., 2003. Searching for seismic scattering off mantle interfaces between 800 and 2000 km depth. Journal of Geophysical Research 108 (2095), 2003. http://dx.doi.org/10.1029/2001JB000286.

Chase, C., 1979. Subduction, the geoid, and lower mantle convection. Nature 282, 464–468. http://dx.doi.org/10.1038/282464a0.

Christensen, U., Hofmann, A., 1994. Segregation of subducted oceanic-crust in the convecting mantle. Journal of Geophysical Research - Solid Earth 99, 19867–19884. http://dx.doi.org/10.1029/93JB03403.

Christensen, U., Yuen, D., 1985. Layered convection induced by phase-transitions. Journal of Geophysical Research - Solid Earth 90, 291–300. http://dx.doi.org/10.1029/JB090iB12p10291.

Coltice, N., Rolf, T., Tackley, P.J., Labrosse, S., 2012. Dynamic causes of the relation between area and age of the ocean floor. Science 336, 335–338.

Conrad, C.P., 2013. The solid earth's influence on sea level. Geological Society of America Bulletin 125, 1027–1052. http://dx.doi.org/10.1130/B30764.1.

Conrad, C.P., Behn, M.D., 2010. Constraints on lithosphere net rotation and asthenospheric viscosity from global mantle flow models and seismic anisotropy. Geochemistry, Geophysics, Geosystems 11, Q05W05. http://dx.doi.org/10.1029/2009GC002970.

Conrad, C.P., Molnar, P., 1997. The growth of Rayleigh–Taylor-type instabilities in the lithosphere for various rheological and density structures. Geophysical Journal International 129, 95–112. http://dx.doi.org/10.1111/j.1365-246X.1997.tb00939.x.

Conrad, C.P., Steinberger, B., Torsvik, T.H., 2013. Stability of active mantle upwelling revealed by net characteristics of plate tectonics. Nature 498, 479–482. http://dx.doi.org/10.1038/nature12203.

Cottaar, S., Romanowicz, B., 2013. Observations of changing anisotropy across the southern margin of the African LLSVP. Geophysical Journal International 195, 1184–1195. http://dx.doi.org/10.1093/gji/ggt285.

Courtillot, V., Davaille, A., Besse, J., Stock, J., 2003. Three distinct types of hotspots in the Earth's mantle. Earth and Planetary Science Letters 205, 295–308. http://dx.doi.org/10.1016/S0012-821X(02)01048-8.

Davaille, A., 1999. Simultaneous generation of hotspots and superswells by convection in a heterogenous planetary mantle. Nature 402, 756–760. http://dx.doi.org/10.1038/45461.

Davies, D.R., Goes, S., Sambridge, M., 2015. On the relationship between volcanic hotspot locations, the reconstructed eruption sites of large igneous provinces and deep mantle seismic structure. Earth and Planetary Science Letters 411, 121–130.

Davies, D.R., Goes, S., Davies, J.H., Schuberth, B.S.A., Bunge, H.-P., Ritsema, J., 2012. Reconciling dynamic and seismic models of Earth's lower mantle: the dominant role of thermal heterogeneity. Earth and Planetary Science Letters 353, 253–269. http://dx.doi.org/10.1016/j.epsl.2012.08.016.

Davies, G.F., 1999. Dynamic Earth: Plates, Plumes and Mantle Convection. Cambridge Univ. Press, New York (458 pp.).

Davies, G.F., 1993. Cooling the core and mantle by plume and plate flow. Geophysical Journal International 115, 132–146.

Davies, G.F., 1989. Mantle convection model with a dynamic plate: topography, heat flow and gravity anomalies. Geophysical Journal International 98, 461–464.

Davies, G.F., 1988a. Ocean bathymetry and mantle convection: 1. Large-scale flow and hotspots. Journal of Geophysical Research 93, 10,467–10,489.

Davies, G.F., 1988b. Role of the lithosphere in mantle convection. Journal of Geophysical Research 93 (B9), 10451–10466. http://dx.doi.org/10.1029/JB093iB09p10451.

Davies, G.F., 1984. Geophysical and isotopic constraints on mantle convection: an interim synthesis. Journal of Geophysical Research 89, 6017–6040.

Davies, G.F., Pribac, F., 1993. Mesozoic seafloor subsidence and the Darwin rise, past and present. The Mesozoic Pacific: Geology, Tectonics, and Volcanism. American Geophysical Union, pp. 39–52.

Davies, G., Richards, M., 1992. Mantle convection. Journal of Geology 100, 151–206.

De Koker, N., Steinle-Neumann, G., Vlcek, V., 2012. Electrical resistivity and thermal conductivity of liquid Fe alloys at high P and T, and heat flux in Earth's core. Proceedings of the National Academy of Sciences of the United States of America 109, 4070–4073. http://dx.doi.org/10.1073/pnas.1111841109.

Domeier, M., Torsvik, T.H., 2014. Plate tectonics in the late Paleozoic. Geoscience Frontiers 5, 303–350. http://dx.doi.org/10.1016/j.gsf.2014.01.002.

Dziewonski, A., 1984. Mapping the lower mantle — determination of lateral heterogeneity in P-velocity up to degree and order-6. Journal of Geophysical Research 89, 5929–5952.

Dziewonski, A., Hager, B., Oconnell, R., 1977. Large-scale heterogeneities in lower mantle. Journal of Geophysical Research 82, 239–255. http://dx.doi.org/10.1029/JB082i002p00239.

England, P., Molnar, P., 1997. Active deformation of Asia: from kinematics to dynamics. Science 278, 647–650.

Ernst, R., Bleeker, W., 2010. Large igneous provinces (LIPs), giant dyke swarms, and mantle plumes: significance for breakup events within Canada and adjacent regions from 2.5 Ga to the Present. Canadian Journal of Earth Sciences 47, 695–739. http://dx.doi.org/10.1139/E10-025.

Evans, D.A.D., 2003. True polar wander and supercontinents. Tectonophysics 362, 303–320.

Fei, Y., Van Orman, J., Li, J., van Westrenen, W., Sanloup, C., et al., 2004. Experimentally determined postspinel transformation boundary in Mg2SiO4 using MgO as an internal pressure standard and its geophysical implications. Journal of Geophysical Research 109, B02305.

Flament, N., Gurnis, M., Müller, R.D., 2013. A review of observations and models of dynamic topography. Lithosphere 5, 189–210.

Flemming, N., Roberts, D., 1973. Tectono-eustatic changes in sea-level and seafloor spreading. Nature 243, 19–22. http://dx.doi.org/10.1038/243019a0.

Flesch, L.M., Holt, W.E., Haines, A.J., Shen-Tu, B., 2000. Dynamics of the Pacific-North American plate boundary in the western United States. Science 287, 834–836.

Flowers, R.M., Ault, A.K., Kelley, S.A., Zhang, N., Zhong, S., 2012. Epeirogeny or eustasy? Paleozoic–Mesozoic vertical motion of the North American continental interior from thermochronometry and implications for mantle dynamics. Earth and Planetary Science Letters 317, 436–445. http://dx.doi.org/10.1016/j.epsl.2011.11.015.

Flowers, R.M., Schoene, B., 2010. (U–Th)/He thermochronometry constraints on unroofing of the eastern Kaapvaal craton and significance for uplift of the southern African Plateau. Geology 38, 827–830. http://dx.doi.org/10.1130/G30980.1.

Foley, B., Becker, T.W., 2009. Generation of plate-like behavior and mantle heterogeneity from a spherical, visco-plastic convection model. Geochemistry, Geophysics, Geosystems 10, Q08001. http://dx.doi.org/10.1029/2009GC002378.

Fukao, Y., Obayashi, M., 2013. Subducted slabs stagnant above, penetrating through, and trapped below the 660 km discontinuity. Journal of Geophysical Research - Solid Earth 118, 5920–5938. http://dx.doi.org/10.1002/2013JB010466.

Fukao, Y., Obayashi, M., Nakakuki, T., 2009. Stagnant slab: a review. Annual Review of Earth and Planetary Sciences 37, 19–46. http://dx.doi.org/10.1146/annurev.earth.36.031207.124224.

Fukao, Y., Widiyantoro, S., Obayashi, M., 2001. Stagnant slabs in the upper and lower mantle transition region. Reviews of Geophysics 39, 291–323. http://dx.doi.org/10.1029/1999RG000068.

Garnero, E.J., 2000. Heterogeneity of the lowermost mantle. Annual Review of Earth and Planetary Sciences 28, 509–537. http://dx.doi.org/10.1146/annurev.earth.28.1.509.

Garnero, E.J., McNamara, A.K., 2008. Structure and dynamics of Earth's lower mantle. Science 320, 626–628. http://dx.doi.org/10.1126/science.1148028.

Gerault, M., Becker, T.W., Kaus, B.J.P., Faccenna, C., Moresi, L., Husson, L., 2012. The role of slabs and oceanic plate geometry in the net rotation of the lithosphere, trench motions, and slab return flow. Geochemistry, Geophysics, Geosystems 13, Q04001. http://dx.doi.org/10.1029/2011GC003934.

Glatzmaier, G.A., Coe, R.S., Hongre, L., Roberts, P.H., 1999. The role of the Earth's mantle in controlling the frequency of geomagnetic reversals. Nature 401, 885–890. http://dx.doi.org/10.1038/44776.

Goes, S., Eakin, C.M., Ritsema, J., 2013. Lithospheric cooling trends and deviations in oceanic PP-P and SS-S differential traveltimes. Journal of Geophysical Research - Solid Earth 118, 996–1007. http://dx.doi.org/10.1002/jgrb.50092.

Goldreich, P., Toomre, A., 1969. Some remarks on polar wandering. Journal of Geophysical Research 74, 2555–2567.

Gomi, H., Ohta, K., Hirose, K., Labrosse, S., Caracas, R., Verstraete, M.J., Hernlund, J.W., 2013. The high conductivity of iron and thermal evolution of the Earth's core. Physics of the Earth and Planetary Interiors 224, 88–103. http://dx.doi.org/10.1016/j.pepi.2013.07.010.

Gonnermann, H.M., Mukhopadhyay, S., 2009. Preserving noble gases in a convecting mantle. Nature 459. http://dx.doi.org/10.1038/nature08018 (560-U88).

Gordon, R., Jurdy, D., 1986. Cenozoic global plate motions. Journal of Geophysical Research - Solid Earth and Planets 91, 2389–2406. http://dx.doi.org/10.1029/JB091iB12p12389.

Grand, S.P., 1994. Mantle shear structure beneath the America and surrounding oceans. Journal of Geophysical Research - Solid Earth 99, 11591–11621. http://dx.doi.org/10.1029/94JB00042.

Grand, S.P., 2002. Mantle shear-wave tomography and the fate of subducted slabs. Philosophical Transactions of the Royal Society A: Mathematical, Physical and Engineering Sciences 360, 2475–2491. http://dx.doi.org/10.1098/rsta.2002.1077.

Grand, S.P., van der Hilst, R.D., Widiyantoro, S., 1997. Global seismic tomography: a snapshot of convection in the Earth. GSA Today 7, 1–7.

Grigne, C., Labrosse, S., Tackley, P.J., 2005. Convective heat transfer as a function of wavelength: implications for the cooling of the Earth. Journal of Geophysical Research 110, B03409. http://dx.doi.org/10.1029/2004JB003376.

Gurnis, M., 1993. Phanerozoic marine inundation of continents driven by dynamic topography above subducting slabs. Nature 364, 589–593.

Gurnis, M., 1988. Large-scale mantle convection and the aggregation and dispersal of supercontinents. Nature 332, 695–699.

Hager, B.H., Richards, M.A., 1989. Long-wavelength variations in Earth's geoid — physical models and dynamical implications. Philosophical Transactions of the Royal Society of London, Series A 328, 309–327.

Hager, B.H., Clayton, R.W., Richards, M.A., Comer, R.P., Dziewonski, A.M., 1985. Mantle heterogeneity, dynamic topography and the geoid. Nature 313, 541–545.

Hager, B.H., O'Connell, R.J., 1979. Kinematic models of large-scale flow in the Earth's mantle. Journal of Geophysical Research 84, 1031–1048.

Hallam, A., 1984. Pre-quaternary sea-level changes. Annual Review of Earth and Planetary Sciences 12, 205–243.

Han, L., Gurnis, M., 1996. How valid are dynamic models of subduction and convection when plate motions are prescribed? Physics of the Earth and Planetary Interiors 110, 235–246.

Hansen, U., Yuen, D.A., Kroening, S.E., Larsen, T.B., 1993. Dynamic consequences of depth-dependent thermal expansivity and viscosity on mantle circulations and thermal structure. Physics of the Earth and Planetary Interiors 77, 205–223.

Harder, H., 2000. Mantle convection and the dynamic geoid of Mars. Geophysical Research Letters 27, 301–304.

Hernlund, J.W., McNamara, A.K., 2015. The core-mantle boundary region. In: Bercovici, D., Schubert, G. (Eds.), Treatise on Geophysics, vol. 8: Mantle Dynamics. Elsevier Ltd., Oxford, pp. 461–519.

Hernlund, J.W., 2010. On the interaction of the geotherm with a post-perovskite phase transition in the deep mantle. Physics of the Earth and Planetary Interiors 180 (3-4), 222–234.

Hernlund, J.W., Thomas, C., Tackley, P.J., 2005. A doubling of the post-perovskite phase boundary and structure of the Earth's lowermost mantle. Nature 434, 882–886.

Hernlund, J.W., Houser, C., 2008. On the distribution of seismic velocities in Earth's deep mantle, Earth Planet. Science Letters 265, 423–437.

He, Y., Wen, L., 2012. Geographic boundary of the "Pacific Anomaly" and its geometry and transitional structure in the north. Journal of Geophysical Research 117, B09308. http://dx.doi.org/10.1029/2012JB009436.

He, Y., Wen, L., 2009. Structural features and shear-velocity structure of the "Pacific Anomaly". Journal of Geophysical Research 114, B02309. http://dx.doi.org/10.1029/2008JB005814.

Hewitt, J.M., McKenzie, D.P., Weiss, N.O., 1975. Dissipative heating in convective flows. Journal of Fluid Mechanics 68, 721–738.

Hill, R.I., Campbell, I.H., Davies, G.F., Griffiths, R.W., 1992. Mantle plumes and continental tectonics. Science 256, 186–193.

Hoeink, T., Lenardic, A., 2008. Three-dimensional mantle convection simulations with a low-viscosity asthenosphere and the relationship between heat flow and the horizontal length scale of convection. Geophysical Research Letters 35, L10304.

Hoffman, P.F., 1991. Did the breakout of Laurentia turn Gondwanaland inside-out? Science 252, 1409–1412.

Hofmann, A.W., 1997. Mantle geochemistry: the message from oceanic volcanism. Nature 385, 219–229.

Houser, C., Masters, G., Shearer, P., Laske, G., 2008. Shear and compressional velocity models of the mantle from cluster analysis of long-period waveforms. Geophysical Journal International 174, 195–212.

Huang, J.S., Zhong, S.J., 2005. Sublithospheric small-scale convection and its implications for residual topography at old ocean basins and the plate model. Journal of Geophysical Research 110, B05404. http://dx.doi.org/10.1029/2004JB003153.

Ishii, M., Tromp, J., 1999. Normal-mode and free-air gravity constraints on lateral variations in velocity and density of Earth's mantle. Science 285, 1231–1236.

Iwamori, H., Nakamura, H., 2015. Isotopic heterogeneity of oceanic, arc and continental basalts and its implications for mantle dynamics. Gondwana Research 27, 1131–1152. http://dx.doi.org/10.1016/j.gr.2014.09.003.

Jadamec, M.A, Billen, M.I., 2010. Reconciling surface plate motions with rapid three-dimensional mantle flow around a slab edge. Nature 465, 338–342.

Jarvis, G.T., McKenzie, D.P., 1980. Convection in a compressible fluid with infinite Prandtl number. Journal of Fluid Mechanics 96, 515–583.

Jaupart, C., Parsons, B., 1985. Convective instabilities in a variable viscosity fluid cooled from above. Physics of the Earth and Planetary Interiors 39, 14–32.

Jellinek, A.M., Manga, M., 2004. Links between long-lived hotspots, mantle plumes, D″ and plate tectonics. Reviews of Geophysics 42, RG3002. http://dx.doi.org/10.1029/2003RG000144.

Karason, H., van der Hilst, R.D., 1999. Compositional heterogeneity in the bottom kilometers of Earth's mantle: toward a hybrid convection model. Science 283, 1885–1888.

Karato, S., 1993. Importance of anelasticity in the interpretation of seismic tomography. Geophysical Research Letters 20, 1623–1626.

Ke, Y., Solomatov, V.S., 2006. Early transient superplumes and the origin of the Martian crustal dichotomy. Journal of Geophysical Research 111, E10001. http://dx.doi.org/10.1029/2005JE002631.

Kellogg, L.H., Hager, B.H., van der Hilst, R.D., 1999. Compositional stratification in the deep mantle. Science 283, 1881–1884.

Kennett, B.L.N., Widiyantoro, S., van der Hilst, R.D., 1998. Joint seismic tomography for bulk sound and shear wave speed in the Earth's mantle. Journal of Geophysical Research 12469–12493.

Kominz, M.A., 1984. Oceanic ridge volume and sea-level change — an error analysis. In: Schlee, J.S. (Ed.), Inter-regional unconformities and hydrocarbon accumulation: Tulsa, Oklahoma. American Association of Petroleum Geologists Memoir 36, pp. 109–127.

Korenaga, J., 2008. Urey ratio and the structure and evolution of Earth's mantle. Reviews of Geophysics 46, RG2007. http://dx.doi.org/10.1029/2007RG000241.

King, S.D., Gable, C.W., Weinstein, S.A., 1992. Models of convection-driven tectonic plates: a comparison of methods and results. Geophysical Research Letters 109, 481–487.

Koschmieder, E.L., 1993. Benard Cells and Taylor vortices. Cambridge University Press, p. 337.

Labrosse, S., Hernlund, J.W., Coltice, N., 2007. A crystallizing dense magma ocean at the base of the Earth's mantle. Nature 450, 866–869.

Labrosse, S., 2002. Hotspots, mantle plumes and core heat loss, Earth Planet. Science Letters 199, 147–156.

Lay, T., Garnero, E.J., 2007. Reconciling the post-perovskite phase with seismological observations of lowermost mantle structure. In: Hirose, K., Brodholt, J., Lay, T., Yuen, D. (Eds.), Post-Perovskite: The Last Mantle Phase Transition. American Geophysical Union, Monograph, pp. 129–153.

Lay, T., Helmberger, D.V., 1983. A shear velocity discontinuity in the lower mantle. Geophysical Research Letters 10, 63–66.

Lay, T., Hernlund, J., Buffett, B.A., 2008. Core-mantle boundary heat flow. Nature Geoscience 1, 25–32.

Lay, T., Hernlund, J., Garnero, E.J., Thorne, M.S., 2006. A post-perovskite lens and D″ heat flux beneath the central Pacific. Science 314, 1272–1276. http://dx.doi.org/10.1126/science.1133280.

Lay, T., Williams, Q., Garnero, E.J., 1998. The core-mantle boundary layer and deep earth dynamics. Nature 392, 461–468.

Lenardic, A., Richards, M.A., Busse, F.H., 2006. Depth-dependent rheology and the horizontal length scale of mantle convection. Journal of Geophysical Research - Solid Earth 111, B07404. http://dx.doi.org/10.1029/2005JB003639.

Lenardic, A., Moresi, L.-N., Jellinek, A.M., O'Neill, C., Cooper, C.M., Lee, C.T., 2011. Continents, super-continents, mantle thermal mixing, and mantle thermal isolation: theory, numerical simulations, and laboratory experiments. Geochemistry, Geophysics, Geosystems 12, Q10016. http://dx.doi.org/10.1029/2011GC003663.

Leng, W., Zhong, S.J., 2008. Controls on plume heat flux and plume excess temperature. Journal of Geophysical Research 113, B04408. http://dx.doi.org/10.1029/2007JB005155.

Lerch, F.J., Klosko, S.M., Patel, G.B., 1983. A Refined Gravity Model from Lageos (GEML2), NASA Technical Memorandum 84986. Goddard Space Flight Center, Greenbelt/Maryland.
Li, M.M., McNamara, A.K., Garnero, E.J., 2014. Chemical complexity of hotspots caused by cycling oceanic crust through mantle reservoirs. Nature Geoscience 7, 336–370.
Li, X.D., Romanowicz, B., 1996. Global mantle shear velocity model developed using nonlinear asymptotic coupling theory. Journal of Geophysical Research - Solid Earth 101, 22245–22272. http://dx.doi.org/10.1029/96JB01306.
Li, Z.X., Zhong, S.J., 2009. Supercontinent-superplume coupling, true polar wander and plume mobility: plate dominance in whole-mantle tectonics. Physics of the Earth and Planetary Interiors 176, 143–156. http://dx.doi.org/10.1016/j.pepi.2009.05.004.
Li, Z.X., et al., 2008. Assembly, configuration, and break-up history of Rodinia: a synthesis. Precambrian Research 160 (1–2), 179–210.
Litasov, K.D., Ohtani, E., Sano, A., Suzuki, A., Funakoshi, K., 2005. In situ X-ray diffraction study of postspinel transformation in a peridotite mantle: implication for the 660-km discontinuity. Earth and Planetary Science Letters 238, 311–328.
Lithgow-Bertelloni, C., Richards, M.A., Conrad, C.P., Griffiths, R.W., 2001. Plume generation in natural thermal convection at high Rayleigh and Prandtl numbers. Journal of Fluid Mechanics 434, 1–21.
Lithgow-Bertelloni, C., Richards, M.A., 1998. The dynamics of Cenozoic and Mesozoic plate motions. Reviews of Geophysics 36, 27–78. http://dx.doi.org/10.1029/97RG02282.
Lithgow-Bertelloni, C., Silver, P.G., 1998. Dynamic topography, plate driving forces and the African superswell. Nature 395, 269–272. http://dx.doi.org/10.1038/26212.
Liu, L.J., Spasojevic, S., Gurnis, M., 2008. Reconstructing Farallon plate subduction beneath North America back to the Late Cretaceous. Science 322, 934–938. http://dx.doi.org/10.1126/science.1162921.
Liu, L.J., Stegman, D.R., 2012. Origin of Columbia River flood basalt controlled by propagating rupture of the Farallon slab. Nature 482. http://dx.doi.org/10.1038/nature10749 (386-U1508).
Liu, X., Zhong, S.J., 2015. The long-wavelength geoid from 3-dimensional spherical models of thermal and thermo-chemical mantle convection. Journal of Geophysical Research - Solid Earth 120. http://dx.doi.org/10.1002/2015JB012016.
Liu, X., Zhong, S.J., 2014. Controls on Long-wavelength Convective Structure and the Geoid from 3D Spherical Mantle Convection Models. Abstract, Workshop for mantle and lithospheric dynamics, Banff, Canada.
Lowman, J.P., Jarvis, G.T., 1996. Continental collisions in wide aspect ratio and high Rayleigh number two-dimensional mantle convection models. Journal of Geophysical Research 101, 25,485–25,497.
Loyd, S.J., Becker, T.W., Conrad, C.P., Lithgow-Bertelloni, C., Corsetti, F.A., 2007. Time-variability in Cenozoic reconstructions of mantle heat flow: plate tectonic cycles and implications for Earth's thermal evolution. Proceedings of the National Academy of Science 104, 14266–14271.
Lynner, C., Long, M.D., 2014. Lowermost mantle anisotropy and deformation along the boundary of the African LLSVP. Geophysical Research Letters 41, 3447–3454. http://dx.doi.org/10.1002/2014GL059875.
Maloof, A.C., Halverson, G.P., Kirschvink, J.L., Schrag, D.P., Weiss, B.P., Hoffman, P.F., 2006. Combined paleomagnetic, isotopic, and stratigraphic evidence for true polar wander from the Neoproterozoic Akademikerbreen Group, Svalbard, Norway. Geological Society of America Bulletin 118, 1099–1124. http://dx.doi.org/10.1130/B25892.1.
Masters, G., Jordan, T., Silver, P., Gilbert, F., 1982. Aspherical Earth structure from fundamental spheroidal-mode data. Nature 298, 609–613. http://dx.doi.org/10.1038/298609a0.
Masters, G., Laske, G., Bolton, H., Dziewonski, A., 2000. The relative behavior of shear velocity, bulk sound speed, and compressional velocity in the mantle: implications for chemical and thermal structure. In: Karato, S.-I., Forte, A., Liebermann, R., Guysters, Stixrude, L. (Eds.), Earth's Deep Interior: Mineral Physics and Tomography From the Atomic to the Global Scale. American Geophysical Union, pp. 63–87.
McNamara, A.K., Zhong, S.J., 2005a. Thermochemical structures beneath Africa and the Pacific Ocean. Nature 437, 1136–1139. http://dx.doi.org/10.1038/nature04066.
McNamara, A.K., Zhong, S.J., 2005b. Degree-1 mantle convection: dependence on internal heating and temperature-dependent rheology. Geophysical Research Letters 32, L01301. http://dx.doi.org/10.1029/2004GL021082.
McNamara, A.K., Zhong, S.J., 2004. The influence of thermochemical convection on the fixity of mantle plumes. Earth and Planetary Science Letters 222, 485–500. http://dx.doi.org/10.1016/j.epsl.2004.03.008.
Mei, S., Suzuki, A.M., Kohlstedt, D.L., Dixon, N.A., Durham, W.B., 2010. Experimental constraints on the strength of the lithospheric mantle. Journal of Geophysical Research - Solid Earth 115, B08204. http://dx.doi.org/10.1029/2009JB006873.
Mitchell, R.N., Kilian, T.M., Evans, D.A.D., 2012. Supercontinent cycles and the calculations of absolute palaeolongitude in deep time. Nature 482, 208–211. http://dx.doi.org/10.1038/nature10800.
Mitrovica, J.X., Forte, A.M., 2004. A new inference of mantle viscosity based upon joint inversion of convection and glacial isostatic adjustment data. Earth and Planetary Science Letters 225, 177–189. http://dx.doi.org/10.1016/j.epsl.2004.06.005.
Mitrovica, J., Beaumont, C., Jarvis, G., 1989. Tilting of continental interiors by the dynamical effects of subduction. Tectonics 8, 1079–1094. http://dx.doi.org/10.1029/TC008i005p01079.
Mittelstaedt, E., Tackley, P.J., 2006. Plume heat flux is much lower than CMB heat flow. Earth and Planetary Science Letters 241, 202–210.
Monin, A., 1991. Planetary evolution and global tectonics. Tectonophysics 199, 149–164. http://dx.doi.org/10.1016/0040-1951(91)90170-W.
Montelli, R., Nolet, G., Dahlen, F.A., Masters, G., Engdahl, E.R., Hung, S.H., 2004. Finite frequency tomography reveals a variety of plumes in the mantle. Science 303, 338–343.
Moresi, L., Solomatov, V., 1998. Mantle convection with a brittle lithosphere: thoughts on the global tectonic styles of the Earth and Venus. Geophysical Journal International 133, 669–682. http://dx.doi.org/10.1046/j.1365-246X.1998.00521.x.
Moresi, L., Solomatov, V., 1995. Numerical investigation of 2D convection with extremely large viscosity variations. Physics of Fluids 7, 2154–2162. http://dx.doi.org/10.1063/1.868465.
Morgan, W.J., 1971. Convection plumes in the lower mantle. Nature 230, 42–43.
Muller, R.D., Sdrolias, M., Gaina, C., Steinberger, B., Heine, C., 2008. Long-term sea-level fluctuations driven by ocean basin dynamics. Science 319, 1357–1362.
Murakami, M., Hirose, K., Sata, N., Ohishi, Y., Kawamura, K., 2004. Phase transition of MgSiO3 perovskite in the deep lower mantle. Science 304, 855–858.
Nakagawa, T., Tackley, P.J., 2014. Influence of combined primordial layering and recycled MORB on the coupled thermal evolution of Earth's mantle and core. Geochemistry, Geophysics, Geosystems 15, 619–633. http://dx.doi.org/10.1002/2013GC005128.
Ni, S.D., Tan, E., Gurnis, M., Helmberger, D., 2002. Sharp sides to the African superplume. Science 296, 1850–1852. http://dx.doi.org/10.1126/science.1070698.
Nyblade, A., Robinson, S., 1994. The African superswell. Geophysical Research Letters 21, 765–768. http://dx.doi.org/10.1029/94GL00631.
Ogg, J., 2012. The geomagnetic polarity time scale. In: Gradstein, F., Ogg, J., Schmitz, M., Ogg, G. (Eds.), The Geologic Time Scale 2012. Elsevier, Amsterdam, pp. 85–128.
Olson, P.L., Coe, R.S., Driscoll, P.E., Glatzmaier, G.A., Roberts, P.H., 2010. Geodynamo reversal frequency and heterogeneous core-mantle boundary heat flow. Physics of the Earth and Planetary Interiors 180, 66–79. http://dx.doi.org/10.1016/j.pepi.2010.02.010.
Olson, P., Deguen, R., Hinnov, L.A., Zhong, S.J., 2013. Controls on geomagnetic reversals and core evolution by mantle convection in the Phanerozoic. Physics of the Earth and Planetary Interiors 214, 87–103. http://dx.doi.org/10.1016/j.pepi.2012.10.003.
Olson, P., Deguen, R., Rudolph, M.L., Zhong, S.J., 2015. Core evolution driven by mantle global circulation. Physics of the Earth and Planetary Interiors http://dx.doi.org/10.1016/j.pepi.2015.03.002.
O'Neill, C., Muller, D., Steinberger, B., 2005. On the uncertainties in hot spot reconstructions and the significance of moving hot spot reference frames. Geochemistry, Geophysics, Geosystems 6, Q04003. http://dx.doi.org/10.1029/2004GC000784.
Panning, M., Romanowicz, B., 2006. A three-dimensional radially anisotropic model of shear velocity in the whole mantle. Geophysical Journal International 167, 361–379. http://dx.doi.org/10.1111/j.1365-246X.2006.03100.x.
Parmentier, E.M., Zhong, S., Zuber, M.T., 2002. Gravitational differentiation due to initial chemical stratification: origin of lunar asymmetry by the creep of dense KREEP? Earth and Planetary Science Letters 201, 473–480. http://dx.doi.org/10.1016/S0012-821X(02)00726-4.
Paulson, A., Zhong, S.J., Wahr, J., 2007. Limitations on the inversion for mantle viscosity from post-glacial rebound. Geophysical Journal International 168, 1195–1209.
Pitman III, W.C., 1978. Relationship between eustasy and stratigraphic sequences of passive margins. Geological Society of America Bulletin 89, 1389–1403.
Pozzo, M., Davies, C., Gubbins, D., Alfe, D., 2012. Thermal and electrical conductivity of iron at Earth's core conditions. Nature 485. http://dx.doi.org/10.1038/nature11031 (355-U99).
Ratcliff, J.T., Tackley, P.J., Schubert, G., Zebib, A., 1997. Transitions in thermal convection with strongly variable viscosity. Physics of the Earth and Planetary Interiors 102, 201–212. http://dx.doi.org/10.1016/S0031-9201(97)00013-7.
Resovsky, J.S., Ritzwoller, M.H., 1999. Regularization uncertainty in density models estimated from normal mode data. Geophysical Research Letters 26, 2319–2322. http://dx.doi.org/10.1029/1999GL900540.
Ribe, N.M., de Valpine, D.P., 1994. The global hotspot distribution and instability of D. Geophysical Research Letters 21, 1507–1510. http://dx.doi.org/10.1029/94GL01168.
Ricard, Y., Fleitout, L., Froidevaux, C., 1984. Geoid heights and lithospheric stresses for a dynamic Earth. Annales Geophysicae 2, 267–286.
Ricard, Y., Doglioni, C., Sabadini, R., 1991. Differential rotation between lithosphere and mantle: a consequence of lateral mantle viscosity variations. Journal of Geophysical Research 96, 8407–8415.
Ricard, Y., Richards, M., Lithgowbertelloni, C., Lestunff, Y., 1993. A geodynamic model of mantle density heterogeneity. Journal of Geophysical Research - Solid Earth 98, 21895–21909. http://dx.doi.org/10.1029/93JB02216.
Richards, M.A., Hager, B., 1984. Geoid anomalies in a dynamic Earth. Journal of Geophysical Research 89, 5987–6002. http://dx.doi.org/10.1029/JB089iB07p05987.
Richards, M.A., Jones, D., Duncan, R., Depaolo, D., 1991. A mantle plume initiation model for the Wrangellia flood-basalt and other oceanic plateaus. Science 254, 263–267. http://dx.doi.org/10.1126/science.254.5029.263.
Richards, M.A., Ricard, Y., Lithgow-Bertelloni, C., Spada, G., Sabadini, R., 1997. An explanation for Earth's long-term rotational stability. Science 275, 372–375.
Richards, M.A., Yang, W.S., Baumgardner, J.R., Bunge, H.P., 2001. Role of a low-viscosity zone in stabilizing plate tectonics: implications for comparative terrestrial planetology. Geochemistry, Geophysics, Geosystems 2. http://dx.doi.org/10.1029/2000GC000115.
Ritsema, J., Deuss, A., van Heijst, H.J., Woodhouse, J.H., 2011. S40RTS: a degree-40 shear-velocity model for the mantle from new Rayleigh wave dispersion, teleseismic traveltime and normal-mode splitting function measurements. Geophysical Journal International 184, 1223–1236. http://dx.doi.org/10.1111/j.1365-246X.2010.04884.x.
Ritsema, J., van Heijst, H.J., Woodhouse, J.H., 2004. Global transition zone tomography. Journal of Geophysical Research 109. http://dx.doi.org/10.1029/2003JB002610.
Ritsema, J., van Heijst, H.J., Woodhouse, J.H., 1999. Complex shear wave velocity structure imaged beneath Africa and Iceland. Science 286, 1925–1928. http://dx.doi.org/10.1126/science.286.5446.1925.
Ritzwoller, M.H., Shapiro, N.M., Zhong, S.J., 2004. Cooling history of the Pacific lithosphere. Earth and Planetary Science Letters 226, 69–84. http://dx.doi.org/10.1016/j.epsl.2004.07.032.

Roberts, J.H., Zhong, S.J., 2006. Degree-1 convection in the Martian mantle and the origin of the hemispheric dichotomy. Journal of Geophysical Research, Planets 111, E06013. http://dx.doi.org/10.1029/2005JE002668.
Romanowicz, B., 2003. Global mantle tomography: progress status in the past 10 years. Annual Review of Earth and Planetary Sciences 31, 303–328.
Rudolph, M.L., Zhong, S., 2013. Does quadrupole stability imply LLSVP fixity? Nature 503, E3–E4. http://dx.doi.org/10.1038/nature12792.
Rudolph, M.L., Zhong, S.J., 2014. History and dynamics of net rotation of the mantle and lithosphere. Geochemistry, Geophysics, Geosystems 15, 3645–3657. http://dx.doi.org/10.1002/2014GC005457.
Schuberth, B.S.A., Zaroli, C., Nolet, G., 2012. Synthetic seismograms for a synthetic Earth: long-period P- and S-wave traveltime variations can be explained by temperature alone. Geophysical Journal International 200, 1393–1412.
Schuberth, B.S.A., Bunge, H.-P., Ritsema, J., 2009. Tomographic filtering of high-resolution mantle circulation models: can seismic heterogeneity be explained by temperature alone? Geochemistry, Geophysics, Geosystems 10, Q05W03. http://dx.doi.org/10.1029/2009GC002401.
Scotese, C.R., 1997. Continental Drift. 7th ed. PALEOMAP Project, Arlington, Texas (79 pp.).
Seton, M., et al., 2012. Global continental and ocean basin reconstructions since 200 Ma. Earth-Science Reviews 113, 212–270.
Shephard, G.E., Bunge, H.P., Schuberth, B.S.A., et al., 2012. Testing absolute plate reference frames and the implications for the generation of geodynamic mantle heterogeneity structure. Earth and Planetary Science Letters 317, 204–217.
Sidorin, I., Gurnis, M., Helmberger, D.V., 1999. Evidence for a ubiquitous seismic discontinuity at the base of the mantle. Science 286, 1326–1331. http://dx.doi.org/10.1126/science.286.5443.1326.
Simons, M., Hager, B.H., 1997. Localization of the gravity field and the signature of glacial rebound. Nature 390, 500–504. http://dx.doi.org/10.1038/37339.
Sleep, N., 1990. Hotspots and mantle plumes — some phenomenology. Journal of Geophysical Research - Solid Earth and Planets 95, 6715–6736. http://dx.doi.org/10.1029/JB095iB05p06715.
Spencer, J.R., Nimmo, F., 2013. Enceladus: an active ice world in the Saturn system. Annual Review of Earth and Planetary Sciences 41, 693–717. http://dx.doi.org/10.1146/annurev-earth-050212-124025.
Sramek, O., Zhong, S.J., 2010. Long-wavelength stagnant lid convection with hemispheric variation in lithospheric thickness: link between Martian crustal dichotomy and Tharsis? Journal of Geophysical Research, Planets 115, E09010. http://dx.doi.org/10.1029/2010JE003597.
Steinberger, B., O'Connell, R.J., 2000. Effects of mantle flow on hotspot motion. In: Richards, M.A., Gordon, R.G., van der Hilst, R.D. (Eds.), The History and Dynamics of Global Plate Motions. AGU, Washington, D. C., pp. 377–398.
Steinberger, B., Torsvik, T.H., 2008. Absolute plate motions and true polar wander in the absence of hotspot tracks. Nature 452. http://dx.doi.org/10.1038/nature06824 (620-U6).
Su, W.J., Dziewonski, A.M., 1997. Simultaneous inversion for 3-D variations in shear and bulk velocity in the mantle. Physics of the Earth and Planetary Interiors 100, 135–156. http://dx.doi.org/10.1016/S0031-9201(96)03236-0.
Su, W., Woodward, R., Dziewonski, A., 1994. Degree-12 model of shear velocity heterogeneity in the mantle. Journal of Geophysical Research - Solid Earth 99, 6945–6980. http://dx.doi.org/10.1029/93JB03408.
Tackley, P., 1993. Effects of strongly temperature-dependent viscosity on time-dependent, 3-dimensional models of mantle convection. Geophysical Research Letters 20, 2187–2190. http://dx.doi.org/10.1029/93GL02317.
Tackley, P.J., 1996a. On the ability of phase transitions and viscosity layering to induce long wavelength heterogeneity in the mantle. Geophysical Research Letters 23, 1985–1988. http://dx.doi.org/10.1029/96GL01980.
Tackley, P.J., 1996b. Effects of strongly variable viscosity on three-dimensional compressible convection in planetary mantles. Journal of Geophysical Research - Solid Earth 101, 3311–3332. http://dx.doi.org/10.1029/95JB03211.
Tackley, P.J., 1998. Three-dimensional simulations of mantle convection with a thermo-chemical basal boundary layer. In: Gurnis, M., Wysession, M.E., Knittle, E., Buffett, B.A. (Eds.), Core-Mantle Boundary Region. Amer. Geophys. Union, Washington, pp. 231–253.
Tackley, P.J., 2000. Self-consistent generation of tectonic plates in timedependent, three-dimensionalmantle convection simulations 2. Strain weakening and asthenosphere. Geochemistry, Geophysics, Geosystems 1, 2000GC000043 http://dx.doi.org/10.1029/2000GC000043.
Tackley, P., Stevenson, D., Glatzmaier, G., Schubert, G., 1993. Effects of an endothermic phase-transition at 670 km depth in a spherical model of convection in the Earths mantle. Nature 361, 699–704. http://dx.doi.org/10.1038/361699a0.
Tan, E., Leng, W., Zhong, S., Gurnis, M., 2011. On the location of plumes and lateral movement of thermochemical structures with high bulk modulus in the 3-D compressible mantle. Geochemistry, Geophysics, Geosystems 12, Q07005. http://dx.doi.org/10.1029/2011GC003665.
Tanimoto, T., 1990. Long-wavelength S-wave velocity structure throughout the mantle. Geophysical Journal International 100, 327–336. http://dx.doi.org/10.1111/j.1365-246X.1990.tb00688.x.
Thorne, M.S., Garnero, E.J., Grand, S.P., 2004. Geographic correlation between hot spots and deep mantle lateral shear-wave velocity gradients. Physics of the Earth and Planetary Interiors 146, 47–63. http://dx.doi.org/10.1016/j.pepi.2003.09.026.
Thurber, C., Ritsema, J., 2007. Theory and observations — seismic tomography and inverse methods. In: Schubert, G. (Ed.), Treatise on Geophysics vol. 1. Elsevier Ltd., Oxford, pp. 323–360.
Torsvik, T.H., 2003. The Rodinia jigsaw puzzle. Science 300, 1379–1381. http://dx.doi.org/10.1126/science.1083469.
Torsvik, T.H., Smethurst, M.A., Burke, K., Steinberger, B., 2006. Large igneous provinces generated from the margins of the large low-velocity provinces in the deep mantle. Geophysical Journal International 167, 1447–1460. http://dx.doi.org/10.1111/j.1365-246X.2006.03158.x.
Torsvik, T.H., Steinberger, B., Cocks, L.R.M., Burke, K., 2008a. Longitude: linking Earth's ancient surface to its deep interior. Earth and Planetary Science Letters 276, 273–283.
Torsvik, T.H., Smethurst, M.A., Burke, K., Steinberger, B., 2008b. Long term stability in deep mantle structure: evidence from the ca. 300 Ma Skagerrak-Centered Large Igneous Province (the SCLIP). Earth Planet. Science Letters 267, 444–452.
Torsvik, T.H., Burke, K., Steinberger, B., Webb, S.J., Ashwal, L.D., 2010. Diamonds sampled by plumes from the core-mantle boundary. Nature 466, 352–355.
Torsvik, T.H., van der Voo, R., Doubrovine, P.V., Burke, K., Steinberger, B., Ashwal, L.D., Tronnes, R.G., Webb, S.J., Bull, A.L., 2014. Deep mantle structure as a reference frame for movements in and on the Earth. Proceedings of the National Academy of Sciences of the United States of America 111, 8735–8740. http://dx.doi.org/10.1073/pnas.1318135111.
Tucker, J.M., Mukhopadhyay, S., Schilling, J.-G., 2012. The heavy noble gas composition of the depleted MORB mantle (DMM) and its implications for the preservation of heterogeneities in the mantle. Earth and Planetary Science Letters 355, 244–254. http://dx.doi.org/10.1016/j.epsl.2012.08.025.
Turcotte, D.L., Schubert, G., 2002. Geodynamics. 2nd ed. Cambridge University Press.
Van der Hilst, R.D., de Hoop, M.V., Wang, P., Shim, S.-H., Ma, P., Tenorio, L., 2007. Seismostratigraphy and thermal structure of Earth's core-mantle boundary region. Science 315, 1813–1817. http://dx.doi.org/10.1126/science.1137867.
Van der Hilst, R.D., Widiyantoro, S., Engdahl, E.R., 1997. Evidence for deep mantle circulation from global tomography. Nature 386, 578–584. http://dx.doi.org/10.1038/386578a0.
Van der Hilst, R., Engdahl, R., Spakman, W., Nolet, G., 1991. Tomographic imaging of subducted lithosphere below northwest Pacific island arcs. Nature 353, 37–43. http://dx.doi.org/10.1038/353037a0.
Van der Voo, R., 1994. True polar wander during the middle Paleozoic. Earth and Planetary Science Letters 122, 239–243. http://dx.doi.org/10.1016/0012-821X(94)90063-9.
van Keken, P.E., Ballentine, C.J., 1999. Dynamical models of mantle volatile evolution and the role of phase transitions and temperature-dependent rheology. Journal of Geophysical Research 104, 7137–7168.
Wang, Y., Wen, L.X., 2004. Mapping the geometry and geographic distribution of a very low velocity province at the base of the Earth's mantle. Journal of Geophysical Research - Solid Earth 109, B10305. http://dx.doi.org/10.1029/2003JB002674.
Warren, J.M., Hirth, G., 2006. Grain size sensitive deformation mechanisms in naturally deformed peridotites. Earth and Planetary Science Letters 248, 438–450. http://dx.doi.org/10.1016/j.epsl.2006.06.006.
Watts, A.B., Zhong, S.J., Hunter, J., 2013. The behavior of the lithosphere on seismic to geologic timescales. Annual Review of Earth and Planetary Sciences 41, 443–468. http://dx.doi.org/10.1146/annurev-earth-042711-105457.
Wen, L.X., Silver, P., James, D., Kuehnel, R., 2001. Seismic evidence for a thermo-chemical boundary at the base of the Earth's mantle. Earth and Planetary Science Letters 189, 141–153. http://dx.doi.org/10.1016/S0012-821X(01)00365-X.
Wieczorek, M.A., Jolliff, B.L., Khan, A., Pritchard, M.E., Weiss, B.P., Williams, J.G., Hood, L.L., Righter, K., Neal, C.R., Shearer, C.K., McCallum, I.S., Tompkins, S., Hawke, B.R., Peterson, C., Gillis, J.J., Bussey, B., 2006. The constitution and structure of the lunar interior. In: Jolliff, B.L., Wieczorek, M.A. (Eds.), New Views of the Moon. Mineralogical Soc Amer, Chantilly, pp. 221–364.
Wolfe, C.J., Solomon, S.C., Laske, G., Collins, J.A., Detrick, R.S., Orcutt, J.A., Bercovici, D., Hauri, E.H., 2009. Mantle shear-wave velocity structure beneath the Hawaiian hot spot. Science 326, 1388–1390.
Woodhouse, J., Dziewonski, A., 1984. Mapping the upper mantle — 3-Dimensional modeling of Earth structure by inversion of seismic waveforms. Journal of Geophysical Research 89, 5953–5986. http://dx.doi.org/10.1029/JB089iB07p05953.
Yoshida, M., Ogawa, M., 2005. Plume heat flow in a numerical model of mantle convection with moving plates, Earth Planet. Science Letters 239, 276–285. http://dx.doi.org/10.1016/j.epsl.2005.09.006.
Yoshida, M., Kageyama, A., 2006. Low-degree mantle convection with strongly temperature- and depth-dependent viscosity in a three-dimensional spherical shell. Journal of Geophysical Research 111, B03412. http://dx.doi.org/10.1029/2005JB003905.
Yoshida, M., Santosh, M., 2011. Supercontinents, mantle dynamics and plate tectonics: a perspective based on conceptual vs. numerical models. Earth-Science Reviews 105 (1-2), 1–24. http://dx.doi.org/10.1016/j.earscirev.2010.12.002.
Yoshida, M., Hamano, Y., 2015. Pangea breakup and northward drift of the Indian subcontinent reproduced by a numerical model of mantle convection. Scientific Reports 5, 8407. http://dx.doi.org/10.1038/srep08407.
Zhang, N., Zhong, S., Flowers, R.M., 2012. Predicting and testing continental vertical motion histories since the Paleozoic. Earth and Planetary Science Letters 317, 426–435. http://dx.doi.org/10.1016/j.epsl.2011.10.041.
Zhang, N., Zhong, S., 2011. Heat fluxes at the Earth's surface and core-mantle boundary since Pangea formation and their implications for the geomagnetic superchrons. Earth and Planetary Science Letters 306, 205–216. http://dx.doi.org/10.1016/j.epsl.2011.04.001.
Zhang, N., Zhong, S., Leng, W., Li, Z.-X., 2010. A model for the evolution of the Earth's mantle structure since the Early Paleozoic. Journal of Geophysical Research - Solid Earth 115, B06401. http://dx.doi.org/10.1029/2009JB006896.
Zhang, N., Zhong, S.J., McNamara, A.K., 2009. Supercontinent formation from stochastic collision and mantle convection models. Gondwana Research 15, 267–275. http://dx.doi.org/10.1016/j.gr.2008.10.002.

Zhang, P., Cohen, R.E., Haule, K., 2015. Effects of electron correlations on transport properties of iron at Earth's core conditions. Nature 517, 605–607.
Zhang, S., Yuen, D.A., 1995. ##The influences of lower mantle viscosity stratification on 3D spherical-shell mantle convection. Earth and Planetary Science Letters 132, 157–166. http://dx.doi.org/10.1016/0012-821X(95)00038-E.
Zhao, D.P., 2004. Global tomographic images of mantle plumes and subducting slabs: insight into deep Earth dynamics. Physics of the Earth and Planetary Interiors 146, 3–34.
Zhong, S.J., Rudolph, M.L., 2015. On the temporal evolution of long-wavelength mantle structure of the Earth mantle since the Early Paleozoic. Geochemistry, Geophysics, Geosystems 16, 1599–1615. http://dx.doi.org/10.1002/2015GC005782.
Zhong, S.J., Watts, A.B., 2013. Lithospheric deformation induced by loading of the Hawaiian Islands and its implications for mantle rheology. Journal of Geophysical Research - Solid Earth 118, 6025–6048. http://dx.doi.org/10.1002/2013JB010408.
Zhong, S.J., McNamara, A., Tan, E., Moresi, L., Gurnis, M., 2008. A benchmark study on mantle convection in a 3-D spherical shell using CitcomS. Geochemistry, Geophysics, Geosystems 9, Q10017. http://dx.doi.org/10.1029/2008GC002048.
Zhong, S.J., 2009. Migration of Tharsis volcanism on Mars caused by differential rotation of the lithosphere. Nature Geoscience 2, 19–23. http://dx.doi.org/10.1038/NGEO392.
Zhong, S.J., Zhang, N., Li, Z.-X., Roberts, J.H., 2007. Supercontinent cycles, true polar wander, and very long-wavelength mantle convection. Earth and Planetary Science Letters 261, 551–564. http://dx.doi.org/10.1016/j.epsl.2007.07.049.
Zhong, S.J., 2006. Constraints on thermochemical convection of the mantle from plume heat flux, plume excess temperature and upper mantle temperature. Journal of Geophysical Research 111, B04409. http://dx.doi.org/10.1029/2005JB003972.
Zhong, S.J., 2001. Role of ocean-continent contrast and continental keels on plate motion, net rotation of lithosphere, and the geoid. Journal of Geophysical Research 106, 703–712.
Zhong, S.J., Zuber, M.T., 2001. Degree-1 mantle convection and the crustal dichotomy on Mars. Earth and Planetary Science Letters 189, 75–84.
Zhong, S.J., Zuber, M.T., Moresi, L., Gurnis, M., 2000a. Role of temperature-dependent viscosity and surface plates in spherical shell models of mantle convection. Journal of Geophysical Research - Solid Earth 105, 11063–11082. http://dx.doi.org/10.1029/2000JB900003.
Zhong, S.J., Parmentier, E.M., Zuber, M.T., 2000b. A dynamic origin for the global asymmetry of lunar mare basalts. Earth and Planetary Science Letters 177, 131–140. http://dx.doi.org/10.1016/S0012-821X(00)00041-8.
Zhong, S.J., Gurnis, M., Moresi, L., 1998. The role of faults, nonlinear rheology, and viscosity structure in generating plates from instantaneous mantle flow models. Journal of Geophysical Research 103, 15255–15268.
Zhong, S.J., Gurnis, M., 1994. The role of plates and temperature-dependent viscosity in phase change dynamics. Journal of Geophysical Research 99, 15903–15917.
Zhong, S.J., Gurnis, M., 1993. Dynamic feedback between an non-subducting raft and thermal convection. Journal of Geophysical Research 98, 12219–12232.
Zhou, H., 1996. A high-resolution P wave model for the top 1200 km of the mantle. Journal of Geophysical Research 101, 27791–27810.
Zuber, M.T., 2001. The crust and mantle of Mars. Nature 412, 220–227. http://dx.doi.org/10.1038/35084163.

Shijie Zhong is a Professor of Physics and Geophysics at the Department of Physics, University of Colorado at Boulder. He received his Ph. D. in Geophysics and Scientific Computing from University of Michigan in 1994.

Xi Liu is a Ph.D. graduate student at the Department of Physics, University of Colorado at Boulder. She received her B.S. in Geophysics from University of Science and Technology of China in 2010.